

SYNTHESIS AND CHARACTERIZATION
OF
TETRACARBONYL[6-FERROCENYL-2,2'-BIPYRIDINE]TUNGSTEN(0)
COMPLEX

A THESIS SUBMITTED TO
THE GRADUATE SCHOOL OF NATURAL AND APPLIED SCIENCES
OF
MIDDLE EAST TECHNICAL UNIVERSITY

BY
PELİN EDİNÇ

IN PARTIAL FULFILLMENT OF THE REQUIREMENTS
FOR
THE DEGREE OF MASTER OF SCIENCE
IN
CHEMISTRY

SEPTEMBER 2005

Approval of the Graduate School of Natural and Applied Sciences

Prof. Dr. Canan Özgen
Director

I certify that this thesis satisfies all the requirements as a thesis for the degree of Master of Science.

Prof. Dr. Hüseyin İşçi
Head of the Department

This is to certify that we have read this thesis and that in our opinion it is fully adequate, in scope and quality, as a thesis for the degree of Master of Science.

Prof. Dr. Saim Özkâr
Supervisor

Examining Committee Members

Prof. Dr. Hüseyin İşçi	(METU, CHEM)	_____
Prof. Dr. Saim Özkâr	(METU, CHEM)	_____
Prof. Dr. M. Ahmet Önal	(METU, CHEM)	_____
Prof. Dr. H. Ceyhan Kayran	(METU, CHEM)	_____
Prof. Dr. Zeynel Kılıç	(Ankara Unv., CHEM)	_____

I hereby declare that all information in this document has been obtained and presented in accordance with academic rules and ethical conduct. I also declare that, as required by these rules and conduct, I have fully cited and referenced all material and results that are not original to this work.

Name, Last Name : Pelin EDİNÇ

Signature :

ABSTRACT

SYNTHESIS AND CHARACTERIZATION OF TETRACARBONYL[6-FERROCENYL-2,2'-BIPYRIDINE]TUNGSTEN(0) COMPLEX

Edinç, Pelin

M.S., Department of Chemistry
Supervisor: Prof. Dr. Saim Özkâr

September 2005, 70 pages

In this study, a bidentate ligand, 6-ferrocenyl-2,2'-bipyridine, was prepared by the reaction of lithiated ferrocene with bipyridine. The ligand was identified by ^1H , ^{13}C - NMR and HMQC and UV-Vis spectroscopies. Then, bidentate molecule was reacted with pentacarbonylbis-(trimethylsilylethyne)tungsten(0). The ligand substitution reaction in CH_2Cl_2 yielded the new complex, tetracarbonyl(6-ferrocenyl-2,2'bipyridine)tungsten(0). The isolated and purified complex was fully characterized by elemental analysis, IR, UV-Vis, MS, ^1H and ^{13}C - NMR spectroscopies. Tetracarbonyl(6-ferrocenyl-2,2'bipyridine)chromium(0) was also formed by ligand substitution reaction of 6-ferrocenyl-2,2'-bipyridine with

pentacarbonyl(THF)chromium(0) which was prepared by photolytic substitution of CO from hexacarbonyl chromium(0) in THF. However, tetracarbonyl(6-ferrocenyl-2,2'-bipyridine)chromium(0) could not be isolated by column chromatography.

Electrochemistry of 6-ferrocenyl-2,2'-bipyridine and tetracarbonyl(6-ferrocenyl-2,2'-bipyridine)tungsten(0) was studied by cyclic voltammetry and controlled potential electrolysis combined with UV-Vis. The ligand exhibits a reversible reduction and a reversible oxidation belonging to bipyridine and ferrocene moieties, respectively. One reversible reduction, two irreversible oxidation and a reversible oxidation were observed for tetracarbonyl(6-ferrocenyl-2,2'-bipyridine)tungsten(0). The reversible reduction was attributed to bipyridine whereas two irreversible oxidations were assigned to tungsten centers and reversible oxidation to iron center.

Keywords: Ferrocene, Bipyridine, Carbonyl, Tungsten, Electrochemistry, Synthesis

.

ÖZ

TETRAKARBONYL[6-FERROSENİL-2,2'-BİPİRİDİN]TUNGSTEN(0) KOMPLEKSİNİN SENTEZİ VE KARAKTERİZASYONU

Edinç, Pelin

Yüksek Lisans, Kimya Bölümü

Tez Yöneticisi: Prof. Dr. Saim Özkâr

Eylül 2005, 70 sayfa

Bu çalışmada, iki dişli ligant olan 6-ferrosenil-2,2'-bipiridin, lithiye ferrosen ve bipiridin tepkimesiyle hazırlandı. Molekül, ^1H , ^{13}C - NMR, HMQC ve UV-Vis teknikleri yardımıyla tanımlandı. Daha sonra bu iki dişli ligant, pentakarbonil(bis(trimetil)silylen)tungsten(0) ile tepkimeye sokuldu. Diklorometanda gerçekleştirilen ligant yerdeğiştirme tepkimesi, tetrakarbonil(6-ferrosenil-2,2'-bipiridin)tungsten(0) kompleksinin oluşumu ile sonuçlandı. Bu yeni kompleks, çözelti ortamından izole edilip saflaştırıldı ve elemental analiz, IR, UV-Vis, MS, ^1H ve ^{13}C - NMR spektroskopileri ile tam olarak tanımlandı. Hekzakarbonilkrom(0) da bir CO ligantının THF içinde fotolitik yerdeğiştirmesiyle elde edilen pentakarbonil(THF)krom(0) ile 6-ferrosenil-2,2'-bipiridin ligantının yerdeğiştirme tepkimesinden de tetrakarbonil(6-ferrosenil-2,2'-bipiridin)krom(0) kompleksinin oluştuğu

gözlendi. Fakat tetrakarbonil(6-ferrosenil-2,2'-bipiridin)krom(0) kompleksi kolon kromatografisi ile izole edilemedi.

6-ferrosenil-2,2'-bipiridin bileşiminin ve tetrakarbonil(6-ferrosenil-2,2'-bipiridin) tungsten(0) kompleksinin elektrokimyası dönüşümlü voltametri ve UV-Vis spektroskopisi ile kombine edilmiş sabit potansiyel elektrolizi ile çalışıldı. Ligant için dönüşümlü voltametrde bipiridine ait bir tersinir indirgenme ile ferrosene ait bir tersinir yükseltgenme gözlemlendi. Komplekste ise, bir tersinir indirgenme, bir tersinir yükseltgenme ve iki tersinmez yükseltgenme gözlemlendi. Tersinir indirgenmenin bipiridine, iki tersinmez yükseltgenmenin tungstene ve tersinir yükseltgenmenin demir atomuna ait olduğu gözlemlendi.

Anahtar kelimeler: Ferrosen, Bipiridin, Karbonil, Tungsten, Elektrokimya, Sentez

To my family

ACKNOWLEDGEMENTS

I would like to express my sincere gratitude to Prof. Dr. Saim Özkâr for his encouragement, never ending support and supervision throughout in this study.

I would like to extend my gratitude to Prof. Dr. M. Ahmet Önal for his close interest and valuable criticism especially in the electrochemistry part of this work.

I would like to thank, C205 group, Ercan Bayram, Fatma Sanem Koçak, Fatma Alper, Cüneyt Kavaklı, Mehmet Zahmakıran, Murat Rakap, Dilek Ayşe Boğa, and Ezgi Keçeli, Önder Metin for their caring and encouragement during my study.

I am grateful to my friends, Özlem Sağıroğlu, Melek Çınar, Çağın Görkem Bingöl and Mehmet Cengizhan Yıldırım for their moral support during this work.

The last but not least, I would like to extend my gratitude to my mother Rezzan, my father, Bülent, my aunt and her husband Sema and İsmail and my grandparents, Nurten and Nejat for their moral support and endless patience.

TABLE OF CONTENTS

PLAGIARISM.....	iii
ABSTRACT.....	iv
ÖZ.....	vi
ACKNOWLEDGEMENTS.....	ix
TABLE OF CONTENTS.....	x
LIST OF TABLES.....	xii
LIST OF FIGURES.....	xiii
CHAPTERS	
1. INTRODUCTION.....	1
2. BONDING.....	12
2.1. Metal-Carbonyl Bonding.....	12
2.2. Metal-Imine Bonding.....	17
2.3. Metal- Alkyne Bonding.....	20
3. EXPERIMENTAL.....	22
3.1. Basic Techniques.....	22
3.2. Physical Measurements.....	26
3.2.1. Infrared Spectra.....	26
3.2.2. NMR Spectra.....	26
3.2.3. Mass Spectra.....	26
3.2.4. Elemental Analysis.....	26
3.2.5. UV-VIS Spectra.....	26
3.2.6. Cyclic Voltammetry.....	26
3.2.7. In Situ-Constant Potential Electrolysis.....	27
3.3. Syntheses.....	28
3.3.1. Synthesis of 6-ferrocenyl-2,2'-bipyridine.....	28

3.3.2.	Synthesis of $W(CO)_5(\eta^2\text{-btmse})$	29
3.3.3.	Synthesis of $W(CO)_4(\text{fcbpy})$	30
3.3.4.	Synthesis of $Cr(CO)_4(\text{fcbpy})$	31
4.	RESULTS AND DISCUSSION	32
4.1.	Synthesis of 6-ferrocenyl-2,2'-bipyridine.....	32
4.2.	Synthesis of Tetracarbonyl(6-ferrocenyl-2,2'- bipyridine)tungsten(0)	42
4.3.	Attempt to synthesize tetracarbonyl(6-ferrocenyl-2,2'- bipyridine) chromium(0).....	61
5.	CONCLUSION	65
	REFERENCES.....	67

LIST OF TABLES

Table 2.1. The CO stretching frequencies of some metal carbonyl complexes, measured in the IR spectra.....	15
Table 2.2. The relation between bond order and stretching frequencies of M-C and C-O bonds.....	16
Table 4.1. The chemical shift differences of protons of fcbpy with respect to free ferrocene and unsubstituted bipyridine.....	39
Table 4.2. The chemical shift differences of carbon atoms of fcbpy with respect to free ferrocene and unsubstituted bipyridine	39
Table 4.3. The vibrational modes and IR bands of $W(CO)_5(\eta^2\text{-btmse})$	43
Table 4.4. The absorption bands and their vibrational modes of $W(CO)_4(\text{fcbpy})$ in CH_2Cl_2	47
Table 4.5. 1H - NMR chemical shifts (δ , ppm) of fcbpy and $W(CO)_4(\text{fcbpy})$, and coordination shift values ($\Delta\delta$, ppm).....	52
Table 4.6. ^{13}C - NMR chemical shifts (δ , ppm) of fcbpy and $W(CO)_4(\text{fcbpy})$, and coordination shift values ($\Delta\delta$, ppm).....	52
Table 4.7. Elemental analysis values and theoretical mass percentages of carbon, nitrogen and hydrogen atoms in $W(CO)_4(\text{fcbpy})$	53
Table 4.8. The molar absorptivity values for each absorption band in $W(CO)_4(\text{fcbpy})$	57
Table 4.9. Vibrational modes and frequencies (cm^{-1}) of $Cr(CO)_4(\text{fcbpy})$ and $W(CO)_4(\text{fcbpy})$ in CH_2Cl_2	64

LIST OF FIGURES

Figure 1.1. The incorrect structure of ferrocene initially proposed by Kealy and Pauson	2
Figure 1.2. The correct structure of ferrocene established by Wilkinson and Woodward	3
Figure 1.3. Suggested structural formula of 6-ferrocenyl-2,2'-bipyridine.....	8
Figure 1.4. Suggested structural formula of $W(CO)_4(fcbpy)$	8
Figure 1.5. The synthesis of fcbpy	9
Figure 1.6. The labile-ligand exchange reaction of $W(CO)_5(\eta^2\text{-btmse})$ with fcbpy.	10
Figure 2.1. Molecular orbital description of CO.....	12
Figure 2.2. Formation of a metal \leftarrow carbon σ - bond, dative bond	13
Figure 2.3. Formation of the metal \rightarrow carbon d_{π} - π^* bond, back-bonding	13
Figure 2.4. Synergic effect of the $M \leftarrow CO$ σ -bonding and $M \rightarrow CO$ π -bonding	14
Figure 2.5. Competition of two ligands for the use of the same d_{π} orbital of the central metal atom.....	16
Figure 2.6. The structure of imine molecule.....	17
Figure 2.7. The molecular orbital diagram of an imine molecule.....	17
Figure 2.8. Molecular orbital description of the metal-imine bonding	18
Figure 2.9. Polarization of the π bond in an imine molecule.....	19
Figure 2.10. A nucleophile attacks the nitrogen atom of the coordinated imine	20
Figure 2.11. Molecular orbital description of the metal-acetylene interaction.....	21

Figure 3.1. The inert gas line	23
Figure 3.2. The standard Schlenk tube	23
Figure 3.3. A schematic diagram showing vacuum line	24
Figure 3.4. The apparatus which is used for performing photochemical reactions	25
Figure 3.5. Cyclic voltammetry cell.....	27
Figure 3.6. Constant potential electrolysis cell; RE: Ag-wire reference electrode; CE: Pt-sieve counter electrode; WE: Pt-wire working electrode.....	28
Figure 4.1. The reaction of lithioferrocene with 2,2'-bipyridine.....	33
Figure 4.2. The suggested structure of 6-ferrocenyl-2,2'-bipyridine	34
Figure 4.3. ¹ H-NMR Spectrum of 6-ferrocenyl-2,2'-bipyridine	35
Figure 4.4. ¹³ C-NMR Spectrum of 6-ferrocenyl-2,2'-bipyridine.	37
Figure 4.5. HMQC spectrum of 6-ferrocenyl-2,2'-bipyridine.	38
Figure 4.6. The UV-VIS spectrum of 6-ferrocenyl-2,2'-bipyridine in CH ₂ Cl ₂ , taken at room temperature.	40
Figure 4.7. Cyclic voltammogram of 6-ferrocenyl-2,2'-bipyridine in CH ₂ Cl ₂ , taken at room temperature. Electrolyte: tetrabutylammonium tetrafluoroborate. Reference electrode: SCE.....	41
Figure 4.8. The UV-VIS electronic absorption spectra of 6-ferrocenyl-2,2'-bipyridine recorded during its electrolytic oxidation in CH ₂ Cl ₂ solution Electrolyte; tetrabutylammonium tetrafluoroborate.....	41
Figure 4.9. Bis-(trimethyl)silylethyne (btmse)	42
Figure 4.10. The IR Spectrum W(CO) ₅ (η ² -btmse) in CH ₂ Cl ₂ taken at room temperature.....	44
Figure 4.11. Symmetry coordinates for the CO stretching vibrational modes in W(CO) ₅ (η ² -btmse).	44
Figure 4.12. The FTIR spectrum taken 1 hour after the beginning of the thermal substitution of W(CO) ₅ (η ² -btmse) with fcbpy in CH ₂ Cl ₂ taken at room temperature.....	45
Figure 4.13. The FTIR spectrum of W(CO) ₄ (fcbpy).....	46
Figure 4.14. The symmetry coordinates for the CO stretching vibrational modes in the W(CO) ₄ (fcbpy)	47

Figure 4.15. $W(CO)_4(fcbpy)$ structure.....	48
Figure 4.16. 1H -NMR spectrum of $W(CO)_4(fcbpy)$ in CD_2Cl_2	49
Figure 4.17. ^{13}C -NMR spectrum of $W(CO)_4(fcbpy)$ CD_2Cl_2	51
Figure 4.18. Molecular peak in the mass spectrum of $W(CO)_4(fcbpy)$	54
Figure 4.19. Calculated molecular peak of the complex, $W(CO)_4(fcbpy)$	54
Figure 4.20. Mass spectrum of $W(CO)_4(fcbpy)$	55
Figure 4.21. The UV-VIS spectrum of $W(CO)_4(fcbpy)$ in CH_2Cl_2 , taken at room temperature.....	56
Figure 4.22. The UV-VIS spectra of ligand and complex together in CH_2Cl_2 , taken at room temperature.	57
Figure 4.23. Cyclic voltammogram of $W(CO)_4(fcbpy)$ in CH_2Cl_2 at room temperature. Electrolyte; tetrabutylammonium tetrafluoroborate. Reference electrode: SCE	58
Figure 4.24. Cyclic voltammogram of $W(CO)_4(fcbpy)$ in 1100mV-0mV Electrolyte; tetrabutylammonium tetrafluoroborate. Reference electrode: SCE.....	59
Figure 4.25. The UV-VIS electronic absorption spectra of 1×10^{-4} M $W(CO)_4(fcbpy)$ at -21 °C, recorded during electrolytic oxidation of the complex in CH_2Cl_2 solution containing the electrolyte, 0.1M tetrabutylammonium tetrafluoroborate	60
Figure 4.26. The UV-VIS electronic absorption spectra of 1×10^{-4} M $W(CO)_4(fcbpy)$ at -21 °C, recorded after second electron passage of the complex in CH_2Cl_2 solution containing the electrolyte, 0.1 M tetrabutylammonium tetrafluoroborate	61
Figure 4.27. The IR spectra taken during irradiation of $Cr(CO)_6$ in tetrahydro furan (THF).	62
Figure 4.28. The IR spectra taken during substitution reaction of $Cr(CO)_5(THF)$ with $fcbpy$	63

CHAPTER 1

1. INTRODUCTION

Organometallic compounds are those which contain a metal-carbon bond. The variety of the organic moiety in such compounds is practically infinite, ranging from alkyl substituents to alkenes, alkynes, carbonyls, aromatic and heterocyclic compounds. Although some organometallic compounds have been known for a long time, it is only in the last four or five decades that organometallic chemistry has come into its own and has experienced tremendous growth, both at fundamental level where our insight into the nature of chemical bonds has been broadened by a surprising variety of bonding situations without precedence elsewhere, and in economic impact, such as catalysis.¹

The historical development of organometallic chemistry dates back to third quarter of 1700's. In 1760, the first organometallic compound, 'Cadet's fuming liquid', was synthesized by a French chemist L.C Cadet.² It was an arsenic containing cobalt mineral and a repulsively smelling liquid. The first example of M-C containing compound was later identified as dicacodyl, As_2Me_4 (Grek $\kappa\alpha\kappa\omicron\delta\iota\alpha$ = stink).² In 1827, the first olefin complex, $\text{Na}[\text{PtCl}_3\text{C}_2\text{H}_4]$, known as Zeise's Salt, was synthesized by a Danish Pharmacist W.C.Zeiss.² The first metal carbonyl complex, $[\text{Pt}(\text{CO})\text{Cl}_2]_2$ was obtained by M.P. Schützenberger in 1868.³ Then, in 1888, first binary metal carbonyl which has been used in a commercial process for refining nickel, $\text{Ni}(\text{CO})_4$, was synthesized by L.Mond who is the founder of the English company ICI (Imperial Chemical Industries). Crude nickel has been refined by the Mond carbonylation-decarbonylation process for many decades.^{3,4}



The second metal carbonyl, Fe(CO)_5 , followed in 1891⁵ but further progress was made 30 years later. In 1919, an important compound was produced from the reaction of chromium trichloride and PhMgBr by Hein. The compound was named as polyphenylchromium.⁶ In 1951, bis(cyclopentadienyl) iron or ‘ferrocene’⁷ appeared in a famous *Nature* article published by Kealy and Pauson. They proposed an incorrect σ -complex in which iron bound to a single carbon of each ring (Figure 1.1).

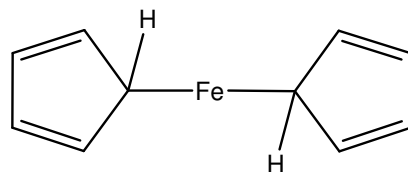


Figure 1.1. The incorrect structure of ferrocene initially proposed by Kealy and Pauson

One year later, Wilkinson and Woodward established the correct formulation as π -complex where iron bound equally to all five carbons in each ring (Figure 1.2).⁸ The industrial chemists were familiar with an orange substance which deposited in iron tubing by cyclopentadiene vapor but its importance was not recognized. By the discovery of ferrocene, it became clear for the first time that transition metals employ bonding modes which are not known in classical organic chemistry. The idea of taking a transition metal in a sandwich between two slices of an organic aromatic molecule was revolutionary.⁹

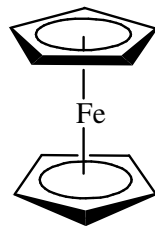


Figure 1.2. The correct structure of ferrocene established by Wilkinson and Woodward

The development of organometallic chemistry occurred unusually rapidly in the second half of the 20th century. This development could be attributed to the relation between general theory of structural chemistry and organometallic chemistry, which contributed to generalization and broadening of certain concepts such as multi center bonding and cluster compounds. The continuing development of structural chemistry (including structural organometallic chemistry) in turn stimulates the synthesis and structural investigations of new organometallic compounds. The application of organometallic compounds in organic synthesis, catalysis, and technology, for example, preparation of metals and their new compounds is another factor that influences the intensification of research in this field.¹⁰

Syntheses of organometallic compounds are carried out by two methods. Reactions using elemental metals and reactions of already formed chemical compounds. The first is done by preparation of Grignard reagents, alkyl lithiums, metal-hydrocarbon reactions such as synthesis of cyclopentadienyl sodium, NaCp, the direct reaction of metals with CO producing metal carbonyls, and metal vapor synthesis using high vacuum and high temperature techniques. The latter synthesis is a more common way of synthesizing organometallic compounds. Some of these reactions are exchange reactions, metal-halogen or hydrogen exchange reactions, addition reactions, oxidative addition reactions, decarbonylation, β -hydrogen eliminations etc.¹¹

In organometallic compounds, bond polarizes as follows: $M^{\delta+}-C^{\delta-}$. As a result, metal or metalloid atom will be susceptible to nucleophilic attack while the carbon atom will be susceptible to electrophilic attack. The polarity of the element-carbon bond is opposite for the other compounds such as with fluorine, oxygen, chlorine etc... Therefore, organometallic compounds contain carbon atoms bonded to elements which are more electropositive than carbon itself. In most organometallic compounds the M-C bond has, to a significant degree, covalent character. Only for alkali and alkaline earth metals' compounds, definite ionic character of M-C bond can be seen. The ionic and covalent contributions to the bond depend on ionization potential of the metal, the size of a resulting ion, the ratio of ionic charge to its radius, and σ -donor, σ -acceptor, π -donor, π -acceptor properties of ligands and their structure.¹⁰

The chemistry of transition metals is accepted as a developing separate field in the organometallics, since it is already extensive and unique. Organotransition metal chemistry is distinguished from the organometallic chemistry of the main group metals by its greater versatility. Although reactive main group organometallics generally add to carbonyl compounds and some activated carbon-carbon double bonds, transition metal compounds frequently react with unactivated, unsaturated organic compounds, often in a catalytic manner. Transition metal compounds have strong tendency to make complexes with various organic and inorganic compounds by sharing more electrons in order to attain the electronic configuration of the next inert gas. An important difference between organotransition chemistry with the chemistry of main group metals is organo transition metals' low tendency to combine with oxygen or its derivatives when compared to main group metals.¹²

The reactions of transition metal complexes bring about at moderate temperatures, usually below 200°C. They combine with different unsaturated molecules such as olefins, acetylenes, carbon monoxide and other reagents in various specific ways in order to form new carbon-carbon bonds. The ultimate aim is to learn how to select transition metal catalysts which will specifically

combine two or more reactive molecules together in any desired cyclic and linear manner.¹²

Carbon monoxide plays an important role in organometallic chemistry since most of the transition metals form compounds, where carbon monoxide acts as ligand. There are three points of interests related to carbonyl compounds. First of all, although the carbonyl ligand is not a very strong base, it could form strong bonds with metals in coordination complexes. Secondly, in these complexes the oxidation state of the metal is usually zero and sometimes appeared as low positive and negative oxidation states, for example, $[\text{V}(\text{CO})_6]$. Thirdly, these complexes obey the 18-electron rule, perhaps 99% of the time.¹³

The vibrational spectra of metal carbonyls are very informative. The CO stretching bands observed in the infrared spectra are to a good approximation specific group frequencies. They are sharp, sensitive to environment, and commonly intense.¹⁴ The vibrations of individual M-CO groups strongly interact¹⁵, so that the observed spectra are rich in well-resolved bands. The number and pattern of these bands are related to the molecular symmetry and geometry while the positions of them are related to bonding.¹⁶ Metal complexes containing one or more CO ligands bound to a single metal atom show one or more intense infrared bands between 2200 and 1800 cm^{-1} .¹⁴ The intensity is large because $d\mu / dr$, the dipole moment change during vibration, is large, thanks to the polarization of the CO on binding to metal.¹⁷

Transition metal carbonyl complexes are the basic starting materials for the synthesis of many organometallic compounds, which are used as catalysts for the reaction of unsaturated hydrocarbons.¹⁸ The octahedral complexes of the type $\text{M}(\text{CO})_6$ (M=Cr, Mo, W) are convenient starting materials for a variety of syntheses. One or more CO ligands can be displaced by Lewis bases such as tertiary phosphines, isonitriles, and amines. Since CO is a good π -accepting ligand, good σ -donors such as tertiary phosphines, amines or ethers usually displace at most three CO groups from $\text{M}(\text{CO})_6$. The hexacarbonyls, $\text{M}(\text{CO})_6$, are

air stable, hydrophobic white crystalline solids which are readily sublimable under vacuum. They are soluble in polar solvents such as THF and CHCl_3 and very slightly soluble in non-polar solvents.¹¹

Organometallic compounds have various applications. They are used as catalyst especially in oxo synthesis. Carbonyls may also be used as catalysts in many processes as hydrosilation, hydrogenation of carbon-carbon multiple bonds, reduction of selected organic compounds, isomerization of unsaturated compounds and polymerization of hydrocarbons. Metal carbonyls are used to obtain high purity metals, their metallic layers for electronics and other technologies.¹⁹

Ferrocene has been called the benzene of modern organometallic chemistry, not only because it was the first pure hydrocarbon derivative of iron to be prepared, but also because it is indissociably linked to the development of organometallic chemistry. Since its accidental discovery in 1951, many derivatives have been synthesized and characterized.²⁰ Ferrocene and ferrocenyl derivatives are of considerable interest in various areas²¹, like asymmetric catalysis, non linear optics²², and electrochemistry²³ due to the quasi-reversible oxidation of iron(II). The planes of the cyclopentadienyl ligand, C_5H_5 (Cp) are perpendicular to the metal ligand bond with all five atoms roughly equidistant from the metal. Both metal-ring plane distances are 1.674\AA .^{24,25} The π -orbitals of the Cp rings and the metal d-orbitals are responsible for the coordination²⁵ and chemical reactivity.²⁰

Ferrocene is a versatile building block for the preparation of compounds with tailor-made properties in many fields, such as organic synthesis, homogeneous catalysis, materials chemistry, and production of fine chemicals due to its high stability and powerful electron releasing ability and well-established methods for its incorporation into more complex structures.²⁶ Generally, ferrocenyl substituents has three distinguishable properties from other purely organic moieties²⁷: (i) unique steric bulk with special steric requirements

due to the cylindrical shape, (ii) electronic stabilization of adjacent electron-deficient centers due to participation of the iron atom in the dispersal of the positive charge,^{28,29} and (iii) chemical stability and reversibility of the ferrocene/ferrocenium redox couple³⁰ has made ferrocene one of the most classical redox couple.

Bipyridine consists of two planar pyridyl rings connected with covalent C-C bond. 2,2'-bipyridine which is the best known isomer, coordinates to metal with both nitrogens yielding the chelate structure.³¹ 2,2'-bipyridine is both a σ -donor and a π -acceptor. The lone electron pair of nitrogen can form σ -bond with the central atom, while the aromatic system can take part in back-bonding. Transition metal ions which are in low oxidation states can be stabilized by bipyridine ligand. Ligands with two or more donor atoms can form a chelate ring with metal atoms. 2,2'-bipyridines, having two nitrogen donor atoms separated by two carbons, form five-membered rings upon coordination to a transition metal center. π -Electron density is delocalized over the chelate ring via the metal-dimine bonding.³²

The chemistry of bipyridyl ligands has been extensively explored over the past two decades or so, because these compounds represent a family of easily accessible, easily modifiable ligands.^{33,34} In addition, they are relatively air-stable, in contrast to other commonly used ligands such as tertiary phosphines, which are prone to oxidation.³³

Ferrocenylpyridines can be considered as imine ligands in bonding to transition metals and thus represent a class of ligands carrying independent redox activity.³⁵ The nitrogen atom can bind a transition metal center through both σ and π interactions using its filled σ orbital (HOMO) and empty π^* orbital (LUMO), respectively, thus, providing a through-bond interaction between the iron atom and the transition metal. The ferrocenyl pyridines were synthesized 40 years ago³⁶ but their coordination properties have not been intensively

described.²⁶ To date, some palladium, platinum and ruthenium complexes have been synthesized.^{33,37}

In this study, we attempted to synthesize and characterize 6-ferrocenyl-2,2'-bipyridine (fcbpy) (Figure 1.3) and its tetracarbonyl tungsten complex (Figure 1.4) for the first time. Since many transition metal complexes of bipyridine are known, ferrocenyl substituted bipyridine is also expected to form stable complexes. It might also be possible to study the electronic communication between tungsten and ferrocene substituted bipyridine moiety due to the coordination of fcbpy molecule to tungsten through π -bonding.

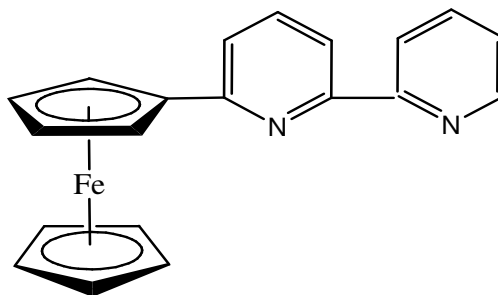


Figure 1.3. Suggested structural formula of 6-ferrocenyl-2,2'-bipyridine

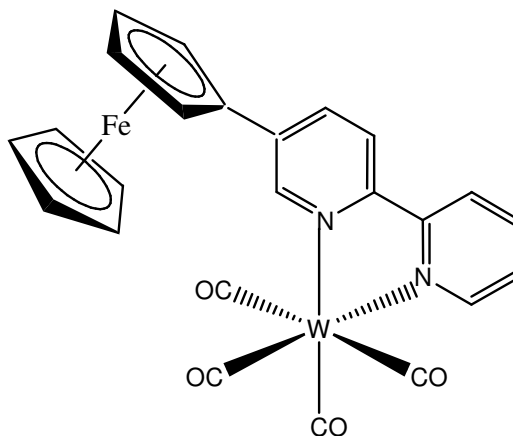


Figure 1.4. Suggested structural formula of $W(CO)_4(fcbpy)$

To synthesize fcbpy, firstly monolithioferrocene was prepared in THF by lithiation of ferrocene by tert-butyllithium at 0°C. Then, it was reacted with excess of 2,2'-bipyridine in diethylether. The synthesis of the ligand is shown in Figure 1.5.

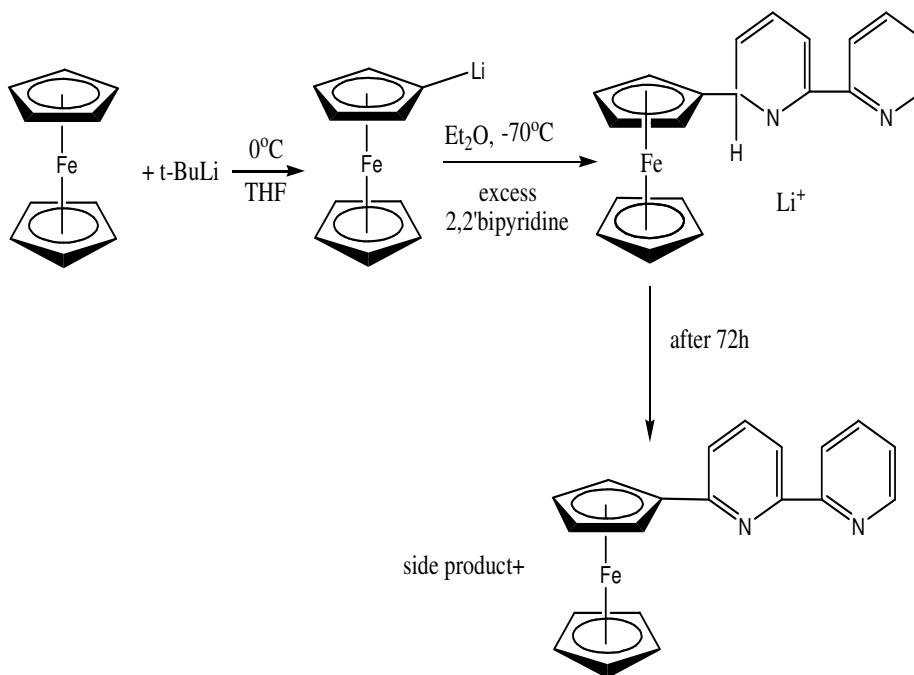


Figure 1.5. The synthesis of fcbpy

Ligand was obtained by crystallization after extraction and column chromatography in order to isolate it from its side product, then, characterized by UV-VIS and NMR spectroscopy techniques. The electrochemical behaviour of the ligand was studied by using cyclic voltammetry and electrode reaction mechanisms were investigated by in-situ UV-VIS measurements.

$\text{W}(\text{CO})_4(\text{fcbpy})$ was prepared by the labile-ligand exchange reaction of the pentacarbonylbis(trimethylsilyl)ethyn tungsten(0), $\text{W}(\text{CO})_5(\eta^2\text{-btmse})$, with fcbpy (Figure 1.6).

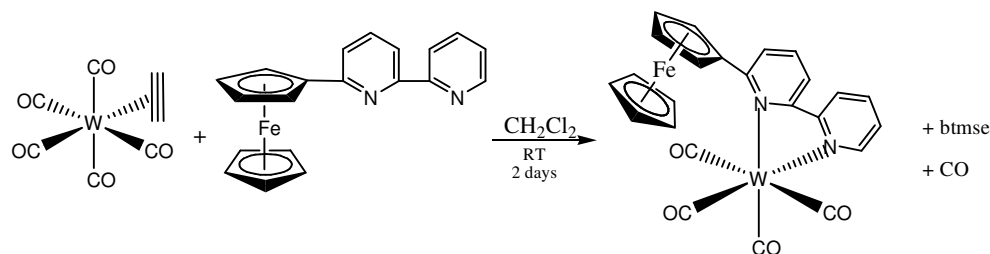


Figure 1.6. The labile-ligand exchange reaction of $W(CO)_5(\eta^2\text{-btmse})$ with fcbpy .

The $W(CO)_4(\text{fcbpy})$ complex was purified by column chromatography after removing the reaction solution under vacuum. The characterization was done by IR, NMR, UV-VIS and mass spectroscopy techniques and elemental analysis. The electrochemical behaviour of the complex was determined by cyclic voltammetry and mechanisms of electrode reactions were studied by in-situ UV-VIS measurements.

The formation of $Cr(CO)_4(\text{fcbpy})$, was performed by ligand substitution reaction of fcbpy with pentacarbonyl(THF)chromium(0) complex which was prepared by photolytic substitution of CO from hexacarbonyl chromium(0) in THF. The reaction was followed by IR spectroscopy but the complex could not be isolated in pure state.

Electrochemistry has been used to study the electronic structure and redox behaviour of organometallic compounds. In order to understand the electron transfer properties of these compounds both spectroscopic and electrochemical studies have to be done. For example, the techniques, cyclic voltammetry and UV-visible electronic absorption spectroscopy must be combined in order to achieve useful information about the electronic structure of organometallic compounds.³⁸

Cyclic voltammetry (CV) is a potential-controlled “reversal” electrochemical experiment. A cyclic potential sweep is imposed on an electrode

and the current response is observed. The potential is varied backwards and forwards between two limits, which lie within the voltammetric range for the solution studied, at constant rate.³⁹ Cyclic voltammetry is a fast technique used for understanding the redox behaviour of organometallic compounds.⁴⁰ The number of electrons involved in electrochemical mechanisms is determined by controlled potential calorimetry and this process is followed by UV-VIS spectroscopy.³⁹

CHAPTER 2

2. BONDING

2.1. Metal-Carbonyl Bonding

Classical ligands such as NH_3 are lewis bases and form donor bonds to lewis acids such as Ni^{2+} via their lone electron pairs; they do not, however, react with zerovalent metals. On the other hand, CO is a very weak base, although its protonated form, the formyl cation CHO^+ , is extremely unstable, CO form adducts with zerovalent metals.¹

This fact can be explained by the molecular orbital description of CO which is shown in Figure 2.1.

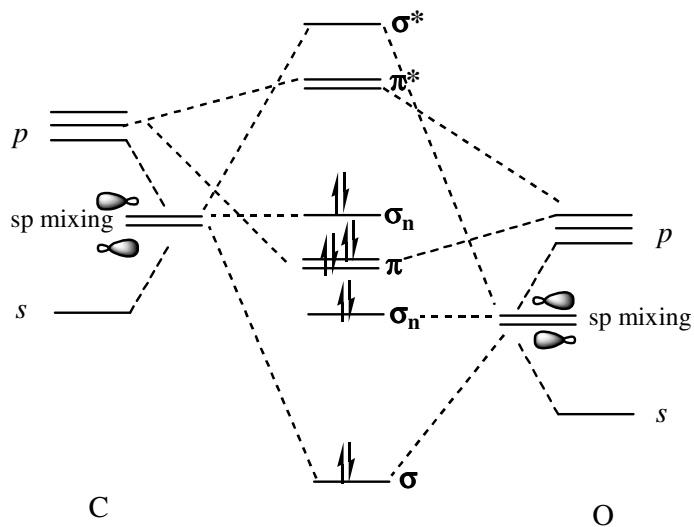


Figure 2.1. Molecular orbital description of CO.

The molecular orbital description of CO shows the existence of a carbon centered lone pair (HOMO) and of degenerate π^* levels (LUMO's). It is known that a ligand interacts with a transition metal by its frontier orbitals. Since frontier orbitals, HOMO and LUMOs are at carbon atom of CO, carbon monoxide is attached to a transition metal through C atom.

The bonding character of carbon monoxide is dual which involves σ -donor and π -acceptor interactions. CO donates the carbon-lone pair through σ -interaction to the vacant metal orbital (Figure 2.2). The LUMOs play a crucial role because they can overlap metal d orbitals that have local π symmetry (Figure 2.3). The π interaction, in other words backbonding, leads to the delocalization of electrons from filled d orbitals on the metal into the empty π^* orbitals on the CO ligands, so the ligand also acts as a π acceptor. The ability of CO to delocalize electron density from the metal accounts for the prevalence of d -metal carbonyls in zero or negative oxidation states.⁴¹



Figure 2.2. Formation of a metal ← carbon σ - bond, dative bond

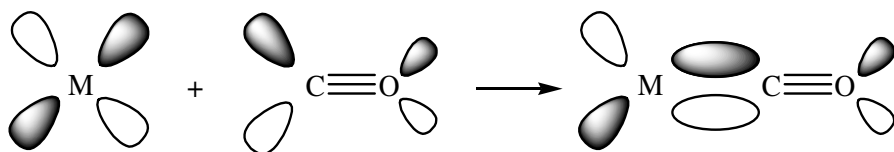


Figure 2.3. Formation of the metal → carbon $d_{\pi} - \pi^*$ bond, back-bonding

This bonding mechanism is synergic (Figure 2.4), since the drift of metal electrons, referred to as back-bonding, into CO orbitals, will tend to make CO as a whole negative, hence to increase its basicity via the σ orbital of carbon; at the same time the drift of electrons to the metal in the σ bond tends to make the CO positive, thus enhancing the acceptor strength of the π orbitals, and vice versa.¹⁶

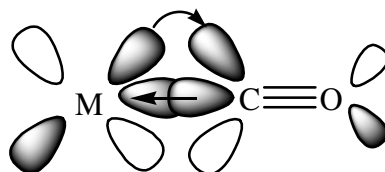


Figure 2.4. Synergic effect of the $M \leftarrow CO$ σ -bonding and $M \rightarrow CO$ π -bonding

Explanations about bonding mechanism of carbon monoxide shows that CO is a strong π acid and thus a powerful electron acceptor which stabilizes the M-CO bond.

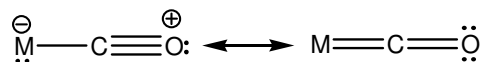
One of the most widely used physical evidence supporting the bonding nature of M-CO bonds is vibrational spectra. According to the preceding description of the bonding, as the extent of back-donation from M to CO increases, the M-C bond becomes stronger and the C=O bond becomes weaker. From the direct comparison of CO stretching frequencies in carbonyl molecules with the stretching frequency of CO itself, qualitative conclusions can be drawn.¹⁶ The frequency (or more properly, the force constant, k) is a measure of the resistance of the bond to displacement of the atoms and hence of the bond strength. Since triple bonds are stronger than double bonds their absorption occurs at higher frequency. This method may also be used to estimate qualitative differences in bond strength. IR data of two isoelectronic series of metal carbonyls are given in the Table 2.1. C-O stretching frequencies in these two series decrease in the order $[Mn(CO)_6]^+ > [Cr(CO)_6] > [V(CO)_6]^-$ and $[Ni(CO)_4] >$

$[\text{Co}(\text{CO})_4]^- > [\text{Fe}(\text{CO})_4]^{-2}$. These qualitative results are consistent with the π -bonding model which was described above. The greater the positive charge on the central metal atom, the less readily the metal can back bond electrons into the π^* orbitals of the carbon monoxide ligands. In contrast, in the carbonylate anions, the metal has a greater electron density to be dispersed and hence π bonding is enhanced.¹³

Table 2.1. The CO stretching frequencies of some metal carbonyl complexes, measured in the IR spectra¹³

Compound	Frequency (cm^{-1})
$\text{Mn}(\text{CO})_6^+$	2090
$[\text{Cr}(\text{CO})_6]$	2000
$[\text{V}(\text{CO})_6]^-$	1860
$[\text{Ni}(\text{CO})_4]$	2060
$[\text{Co}(\text{CO})_4]^-$	1890
$[\text{Fe}(\text{CO})_4]^{-2}$	1790
free CO	2143

The description of the transition metal-CO bond can also be made by the resonance hybrid which leads to a bond order between 1 and 2 for the M-C bond, between 2 and 3 for the C-O bond and to less charge separation which satisfies the electroneutrality principle.³



The relation between bond order and stretching frequencies of M-C and C-O bonds can be seen in Table 2.2

Table 2.2. The relation between bond order and stretching frequencies of M-C and C-O bonds.

	$M(\sigma) \leftarrow CO(\sigma)$ <i>σ-donor interaction</i>	$M(\pi) \rightarrow CO(\pi)$ <i>π-acceptor interaction</i>
Bond order M-C	increases	increases
Bond order C-O	increases	decreases
Stretching frequency ν_{CO}	increases	decreases

Ligands in mutual trans position compete for the electrons of a particular metal d orbital. Two CO groups therefore weaken each other's bond to the same central atom. By replacing a CO group with a ligand which is weaker π -acceptor, the M-CO bond in trans position is strengthened and the C \equiv O bond weakened (Figure 2.5).³

On the other hand, when a weaker donor and a stronger π -acceptor ligand, such as N \equiv O⁺ and CS is replaced with CO group, these ligands compete for the use of the same $d\pi$ orbital of the metal which results in the increase in the frequency of CO stretching.¹⁹

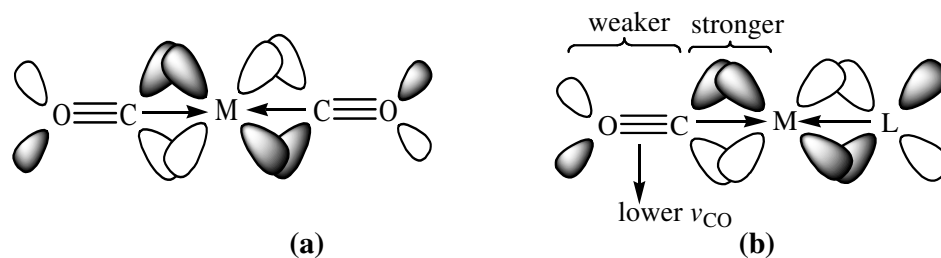


Figure 2.5. Competition of two ligands for the use of the same $d\pi$ orbital of the central metal atom.

- (a) Two carbonyl ligands; equal M-CO π interactions
- (b) Carbonyl ligand and a weaker π -acceptor ligand, L; stronger M-CO π -bonding

2.2. Metal-Imine Bonding

Aldehydes or ketones react with primary amines (RNH_2) to form compounds with a carbon-nitrogen double bond called imines ($\text{RCH}=\text{NR}$ or $\text{R}_2\text{C}=\text{NR}$).⁴² The structure of imine molecule is shown in Figure 2.6.

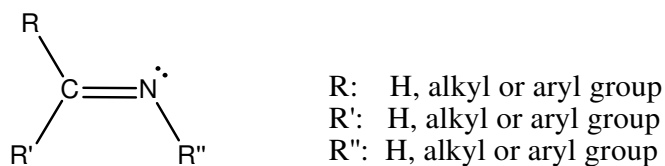


Figure 2.6. The structure of imine molecule

The carbon-nitrogen double bond in an imine molecule consists of a σ -bond and a π -bond. In the MO energy level diagram, (Figure 2.7) there will be two σ -orbitals (bonding and antibonding) and two π -orbitals (bonding and antibonding) for C=N: moiety.

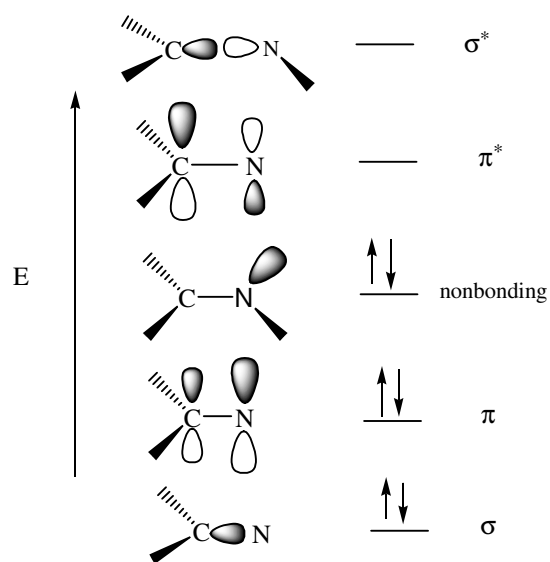


Figure 2.7. The molecular orbital diagram of an imine molecule

Since nitrogen is more electronegative than carbon, it can be deduced that the bonding orbitals are mainly localized on the nitrogen atoms whereas the antibonding orbitals belong mainly to the carbon atom. In addition, there should be one nonbonding σ orbital localized on the nitrogen atom because there are two lone-pair electrons on the nitrogen atom as seen from the structure of the molecule. Totally six electrons (2 from the carbon and 4 from the nitrogen) are available to occupy molecular orbitals of the C=N: moiety of the imine molecule.

The HOMO of the imine molecule is the nonbonding σ orbital, and the LUMO is the antibonding π^* orbital. A strong σ interaction between metal and the imine ligand should be expected because the HOMO, the sigma-symmetry orbital completely localized on the nitrogen, is directed to the $d\sigma$ orbital of the metal along the bond-axis (Figure 2.8(a)). On the other hand, the π bonding takes place to the lower extent in comparison with the σ -bonding because the π^* orbital (LUMO) of imine is mainly localized on the carbon atom, that is, the LUMO has its smaller amplitude on the nitrogen (Figure 2.8 (b)).

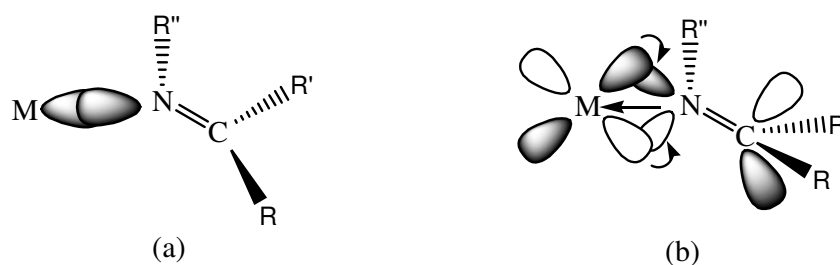


Figure 2.8. Molecular orbital description of the metal-imine bonding

- (a) Metal←imine σ bonding; electrons are donated from nonbonding σ orbital on the nitrogen atom to the empty σ -symmetry d orbital of the metal
- (b) Metal→imine π bonding; the electrons on the $d\pi$ orbital of the metal are backdonated to the empty π^* orbital of the imine.

These σ and π interactions are synergic. If the π^* orbital of the imine molecule were mainly localized on the nitrogen atom, π bonding would have been much stronger; i.e. imines would have π -accepting ability as strong as the CO ligand. However, the imine ligand is a strong σ -donor and weak π -acceptor, depending on the substituents on the carbon and nitrogen atoms, transition metal and the other ligands coordinated to the metal.

In an imine molecule the more electronegative nitrogen atom strongly attracts the electrons of the σ bond and the π bond causing the C=N bond highly polarized; the carbon atom bears a partial positive charge and the nitrogen atom bears a partial negative charge. Polarization of the π -bond can be represented by the following resonance structures (Figure 2.9).

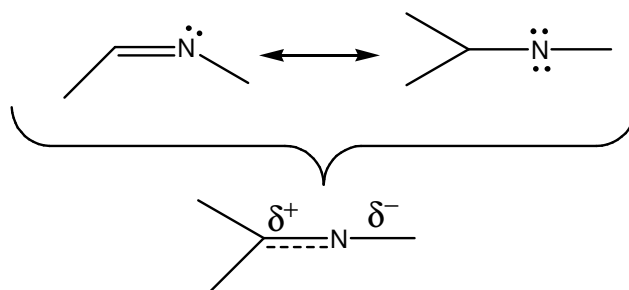


Figure 2.9. Polarization of the π bond in an imine molecule

The nucleophile, which is electron-rich, attacks on the carbon atom bearing a positive charge.

It is often found that imines are stabilized towards hydrolysis by coordination of the nitrogen to a π -bonding transition metal. Of course in the absence of significant π -bonding interactions, ligand polarization is expected to have the opposite effect and activate the imine towards nucleophilic attack⁴³. The polarization of C=N bond of imine is inverted in case of coordination to a transition metal. The electron density of imine is reduced by the donation of non

bonding electrons through σ bonding to the metal. In addition, the electrons backdonated from the $d\pi$ orbital of the metal to the π^* orbital of the imine ligand are localized on the nitrogen very little, so the nitrogen atom bears a partial positive charge; that is, the electron density on the nitrogen lost by σ -bonding cannot be compensated by back bonding. Because the π^* orbital of the imine mainly belongs to the carbon atom, upon coordination to the transition metal, this π^* orbital becomes more populated by electrons, the C=N bond is weakened and the electron density on the carbon atom will increase with respect to the carbon atom of an uncoordinated imine molecule. Consequently, the carbon atom bears a substantial negative charge. On account of this inversion of polarization of C=N bond, the reactivity of imines in nucleophilic addition reactions, where the nucleophile (Nu^-) attacks the carbon atom of the C=N: moiety, is reduced upon coordination to a transition metal. However, they might undergo a nucleophilic attack on the nitrogen atom bearing a partial positive charge as long as the transition metal and the substituent on the nitrogen do not create a significant crowding (Figure 2.10).¹⁹

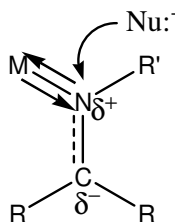


Figure 2.10. A nucleophile attacks the nitrogen atom of the coordinated imine

2.3. Metal- Alkyne Bonding

Alkynes or in other words acetylenes form complexes with transition metals in a similar way to alkenes. However, $\text{C}\equiv\text{C}$ bonds are more reactive and

electron rich when compared to C=C bonds. The characteristic differences between alkynes and alkenes are as follows:

- Alkynes are stronger π -acceptors than alkenes;
- Alkynes have two orthogonal π -systems and can act as 2- as well as 4-electron donor ligands;
- C \equiv C bonds are more reactive than C=C bonds

The molecular orbital description of Dewar⁴⁴, Chatt and Duncanson⁴⁵ explained the metal alkyne bonding. This description consists of two components. The former is σ bond between the π -orbital of the alkyne and σ -type d-orbital on the metal atom occurs. Here, electron is donated by the alkyne. π -Back-bonding exists as a result of the overlap of filled π -type d-orbital of the metal and empty π^* -orbital of the acetylene. Same synergic effect is observed between σ - and π -bonds as in the CO case (Figure 2.11).⁴⁶

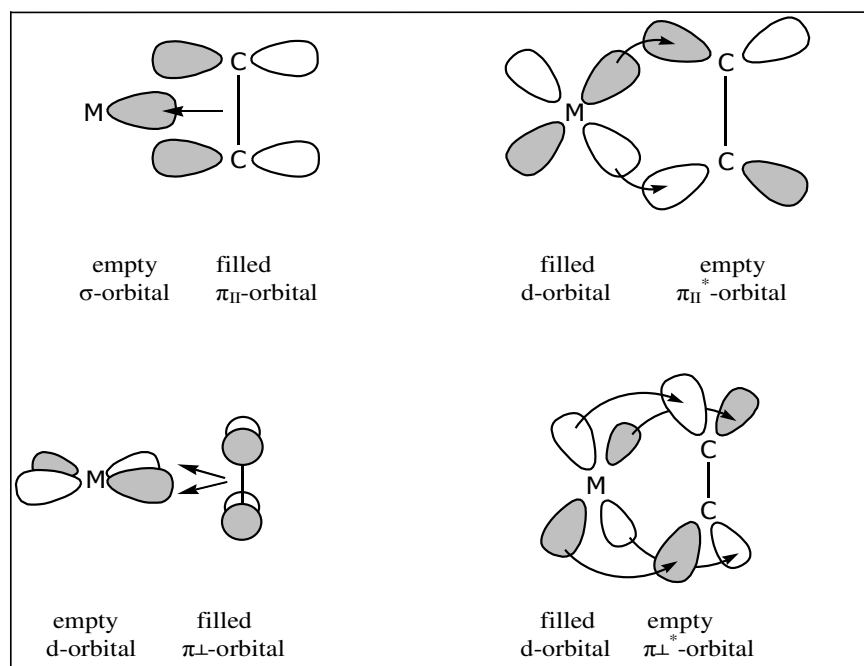


Figure 2.11. Molecular orbital description of the metal-acetylene interaction

CHAPTER 3

3. EXPERIMENTAL

3.1. Basic Techniques

Handling organometallic compounds is a crucial problem since these compounds are air and moisture sensitive and tend to decompose easily when they are in contact with oxygen or in solution. In order to overcome this difficulty, handling of organometallic compounds should be carried out under dry and deoxygenated atmosphere or under vacuum.

In order to obtain appropriate atmosphere, inert gases are used. Pure nitrogen or argon is further purified by using an inert gas line. In this system, the inert gas passes through a catalyst (BASF R3.II, Ludwigshafen, Germany) and is deoxygenated. The temperature of the catalyst is kept at 120°C to be regenerated. Secondly, the gas is passed through molecular sieves to be dried up from its moisture and, lastly, bubbled through glycerine to follow the flowing gas. The inert gas line is shown in Figure 3.1.

Apparatus for handling air-sensitive compounds varies. The simplest and best known technique is the “Schlenk” technique. A Schlenk is a flask which has at least one arm where inert gas can be introduced. Usually a three- or two way stopcock is fitted at the end of the arm. In use, the air in a Schlenk flask should be replaced at least three times by pumping and filling inert gas and all subsequent handling should be carried out under nitrogen flow.¹¹ A standard Schlenk tube is shown in Figure 3.2.

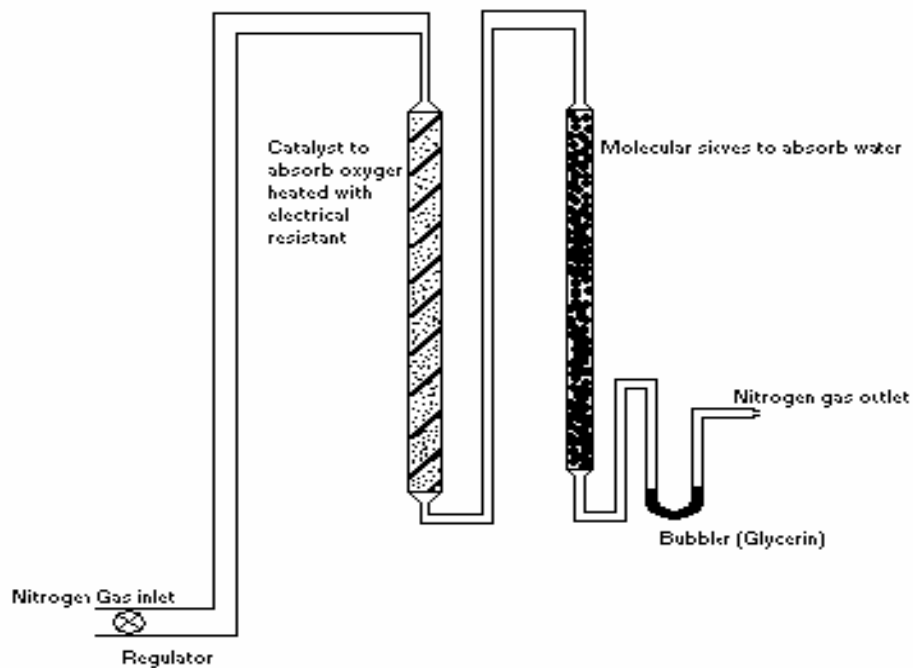


Figure 3.1. The inert gas line

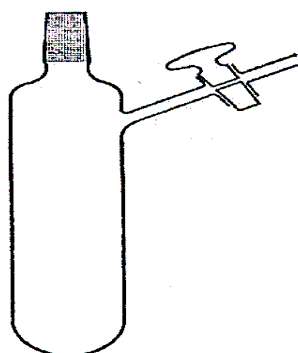


Figure 3.2. The standard Schlenk tube

Vacuum line is another important equipment to be set up for manipulating air-sensitive compounds (Figure 3.3). To obtain a good vacuum, at least one liquid nitrogen trap should be connected between the pump and vacuum system. This technique is used to remove solvents or other volatiles under low pressure.

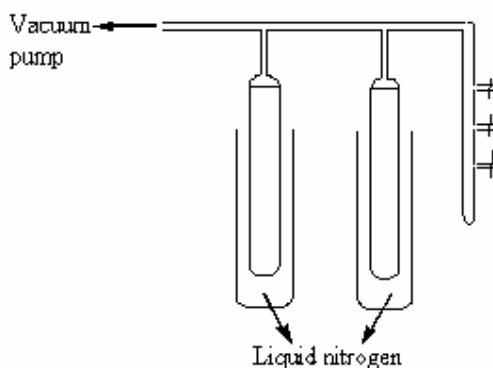


Figure 3.3. A schematic diagram showing vacuum line

Since all reactions are carried out in large excess of solvents compared to reagents, even minor contamination of solvents with water or oxygen may result in low yield of the desired complexes. For this reason, all solvents used in experiments were refluxed over a suitable water holder, such as metallic sodium or phosphorus(V)oxide under nitrogen atmosphere for a few days before use.

Hexacarbonyltungsten(0), n-butyllithium (2.5 M solution in hexane), bis-(trimethyl)silylethyne (btmse), 2,2'-bipyridine were purchased from Aldrich and used without any further purification. Ferrocene was obtained from Merck and used as received. Neutral aluminumoxide (70-230 mesh, Merck) was used for column chromatography in the purification of ligand and complex. Hexane, dichloromethane ($n\text{-CH}_2\text{Cl}_2$) were obtained from Riedel-de Haën, tetrahydrofuran (THF), acetonitrile and toluene were purchased from Aldrich and diethylether

was obtained from Fluka. All of the solvents were refluxed over a suitable water holder (either metallic sodium or phosphorus(V)oxide) under nitrogen atmosphere for a few days before use.

The photochemical reactions were carried out in a special glass apparatus which is shown in Figure 3.4.¹⁹ The inner part (a) is used for immersing the UV lamp (b) (Hg-Tauch Lampe TQ 150 Quartzlampen GmbH, Hanau, West Germany). The photochemical reactions are performed in the outer part (c). The reaction mixture is cooled by circulating water through (d) to (e).

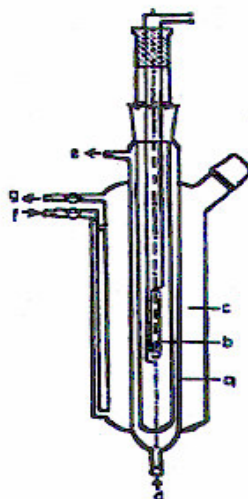


Figure 3.4. The apparatus which is used for performing photochemical reactions

- a- inner part
- b- mercury lamp
- c- outer part
- d- water inlet
- e- water outlet
- f- argon or nitrogen gas inlet
- g- argon or nitrogen gas outlet

3.2. Physical Measurements

3.2.1. Infrared Spectra

The infrared spectra of complexes, $W(CO)_5(btmse)$ and $W(CO)_4(fcbpy)$ were recorded from their n-hexane and dichloromethane solutions, respectively, by using Specac IR-Liquid cell with CaF_2 windows on Nicolet 510 FTIR Spectrometer with OMNIC software.

3.2.2. NMR Spectra

The 1H -NMR and ^{13}C -NMR spectra of the complex, $W(CO)_4(fcbpy)$, and ligand $fcbpy$ were taken from their CD_2Cl_2 (deuterated dichloromethane) solutions on a Bruker-Spectrospin DPX 400 Spectrometer with Avance software. Samples of complexes were prepared under nitrogen atmosphere. TMS was used as an internal reference.

3.2.3. Mass Spectra

Mass spectra of the complex, $W(CO)_4(fcbpy)$, was taken on a Fisons VG Autospec with m-nitrobenzylalcohol as matrix at Colorado State University, Fort Collins, USA.

3.2.4. Elemental Analysis

Elemental analysis of $W(CO)_4(fcbpy)$ was carried out by using LECO CHNS-932 instrument at METU Central Laboratory.

3.2.5. UV-VIS Spectra

The UV-VIS spectra of the ligand and complex were taken from their dichloromethane solutions at room temperature by using Hewlett Packard 8453A Model Diode Array Spectrophotometer with UV-Visible ChemStation software.

3.2.6. Cyclic Voltammetry

The electrochemical experiments of the ligand, $fcbpy$, and complex, $W(CO)_4(fcbpy)$, were performed using HEKA IEEE 488 model potentiostat⁵⁷. The cyclic voltammetry cell is shown in Figure 3.5.

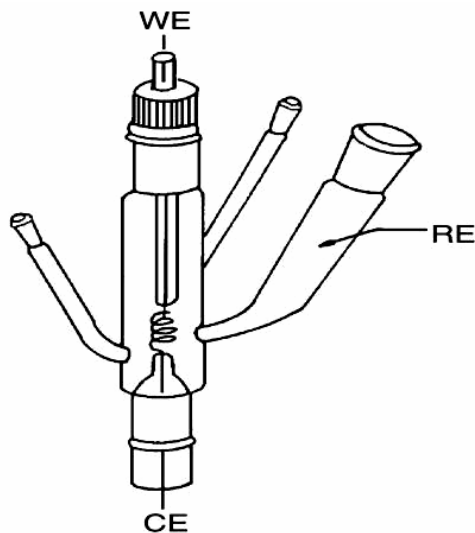


Figure 3.5 Cyclic voltammetry cell

During the experiments, the anhydrous base, tetrabutylammonium tetrafluoroborate, $(n\text{-Bu})_4\text{NBF}_4$ was used as the electrolyte. Nitrogen gas is used during the experiments in order to avoid the interference of the reduction waves of oxygen with those of the compounds. Ag-wire and saturated calomel electrode were used as the reference electrodes whereas platinum disc electrode and the platinum bead electrode were used as counter and working electrodes, respectively.

3.2.7. In Situ-Constant Potential Electrolysis

The oxidation processes of fcbpy and $\text{W}(\text{CO})_4(\text{fcbpy})$ were carried out at 0°C and at -21°C respectively in their CH_2Cl_2 solutions at the peak potentials observed in cyclic voltammetry and determined by Hewlett Packard 8453A Model Diode Array Spectrophotometer with UV-Visible ChemStation software by using a special cell shown in Figure 3.6.⁵⁷ The electrolysis were followed by taking electronic absorption spectra at every 5mC.

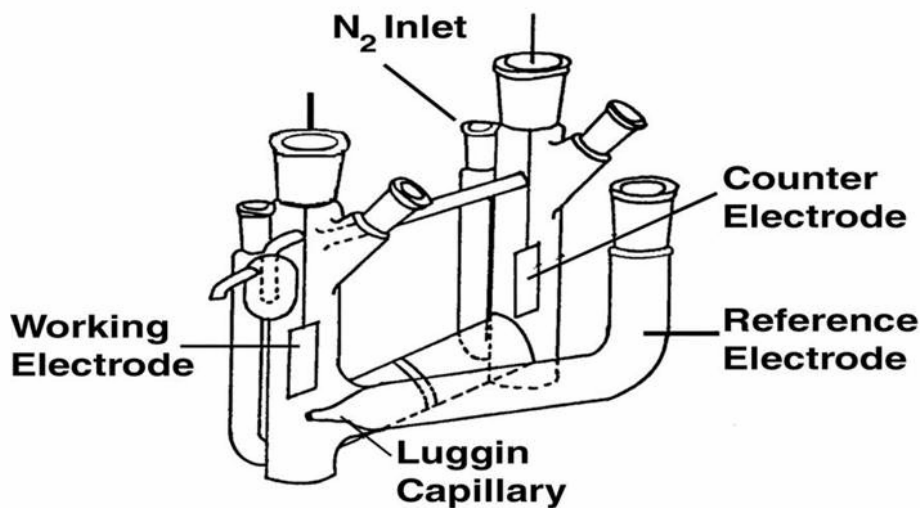


Figure 3.6. Constant potential electrolysis cell; RE: Ag-wire reference electrode; CE: Pt-sieve counter electrode; WE: Pt-wire working electrode

3.3. Syntheses

3.3.1. Synthesis of 6-ferrocenyl-2,2'-bipyridine

The ligand, 6-ferrocenyl-2,2'-bipyridine, shortly fcbpy, was prepared by literature procedure.^{47,48} Firstly, 2.2 g (12 mmol) ferrocene was dissolved at 0 °C in 10 mL tetrahydrofuran (THF) in a schlenk tube. Then, 4.8 mL (12 mmol) of 2.5 M hexane solution of tert-butyllithium was slowly added at 0°C. After standing 15 minutes at 0°C, the solution was warmed up to room temperature. After obtaining a sample of monolithioferrocene/dilithioferrocene by this procedure, THF was removed under vacuum. The remaining solid was suspended in 30 mL diethyl ether and to the cooled stirred solution (-70°C), 1.872 g (12 mmol) of 2,2'-bipyridine was added. After allowing the reaction mixture to warm up slowly to room temperature, it was stirred for three days before being hydrolyzed under aerobic conditions with 30 mL water. The organic layer was separated and the remaining solid in the water phase was further extracted with dichloromethane until the solution became almost colorless. The combined organic fraction was taken to dryness by using rotary evaporator to leave an oily solid. As it was

known from the literature, the major product of the reaction was 6-ferrocenyl-2,2'-bipyridine, column chromatography was performed in order to collect the desired mono-substituted compound. The unreacted ferrocene was separated by using n-hexane as eluent. Then the mixture (50:50) of diethyl ether-dichloromethane was used as eluent in order to collect the orange colored mono-substituted portion. After removing the solvents by using the rotary evaporator, the solid was crystallized from hexane/diethyl ether (4:1). The second orange band which belonged to the side product could not be collected. ¹H-NMR (CDCl₃) δ= 7.36 (d, 1H, J_{4,5} = 7.8 Hz, H-5), δ= 7.65 (t, 1H, H-4), δ= 8.14 (d, 1H, J_{3,4} = 7.7 Hz, J_{5,3}= 0.7 Hz, H-3), δ= 8.62 (d, 1H, J_{6',4'} = 1.7 Hz, J_{6',3'} ~0, H-6'), δ= 7.24 (ddd, 1H, J_{5',6'} = 4.7 Hz, J_{5',4'} = 7.8 Hz, J_{5',3'} = 1.1 Hz, H-5'), δ= 7.78 (dt, 1H, H-4'), δ= 8.51 (d, 1H, H-3'), δ= 4.96 (t, 2H, J_{α-β}=1.8 Hz, α-C₅H₅), δ= 4.35 (t, 2H, β-C₅H₅), δ= 3.98 (s, 5H, unsub-C₅H₅); ¹³C-NMR (CDCl₃) δ=155.60, 154.272 (1C, 1C, C-2, C-2'), δ= 116.66 (1C, C-3), δ=135.78, 135.76 (C-4, C-4'), δ=120.18 (1C, C-3'), δ=119.01 (1C, C-5), δ=122.52 (1C, C-5'), δ=157.45 (1C, C-6), δ= 147.97 (1C, C-6'), δ=68.78 (2C, β-C₅H₅), δ=66.44 (2C, α-C₅H₅), δ=83.13 (1C, *i*-C₅H₅), δ= 68.58 (5C, unsub.-C₅H₅); UV-VIS(CH₂Cl₂) λ(CT) = 234 nm, 286 nm, λ(d-d- Fe(II)) =354 nm, 460 nm; CV(CH₂Cl₂) irrev. red.(bpy)= -1.250, rev. ox. pot(fc)= 0.710.

3.3.2. Synthesis of W(CO)₅(η²-btmse)

W(CO)₅(η²-btmse) was prepared photochemically as described in the literature⁴⁹. 1.0 gram (2.85 mmol) W(CO)₆ and 5.82 gram (34.2 mmol) (CH₃)₃SiC≡CSi(CH₃)₃ (btmse) were dissolved in 200 mL n-hexane in the photochemical reaction vessel. The solution was irradiated for seven hours with stirring at room temperature. Then the solvent was evaporated down to 20 mL at room temperature, under vacuum (10⁻³ mbar). The unreacted W(CO)₆ was crystallized out during the volume reduction and filtered off. The rest of the solvent was completely stripped off and the excess of the ligand was sublimed over a cold finger cooled to -30°C by using cryostat under vacuum. The remaining solid dissolved in 15 mL n-hexane and recrystallized at dry ice

temperature. This yielded yellow-needle like crystals of $W(CO)_5(\eta^2\text{-btmse})$. IR(n-hexane) $\nu(CO)$ = 2079, 1986, 1956, 1939, $\nu(C\equiv C)$ =1906

3.3.3. Synthesis of $W(CO)_4(\text{fcbpy})$

413 mg (0.835 mmol) $W(CO)_5(\eta^2\text{-btmse})$ was dissolved in 15-20 mL dichloromethane at room temperature and 282 mg (0.835 mmol) fcbpy was added. The solution was stirred for 45 hours at room temperature. The solvent was evaporated under vacuum and a dark red colored residue was obtained. Column chromatography was performed under nitrogen atmosphere by using a special glassware. This glassware has two arms at both ends where two or three way stopcocks are fitted in order to introduce the inert gas. The unreacted ligand, fcbpy was eluted by using n-hexane and THF. Then, acetonitrile was used as eluent in order to collect the complex, $W(CO)_4(\text{fcbpy})$. The solvent was removed under vacuum. The remaining solid was purified by using cold-finger in order to collect $W(CO)_6$. IR(CH_2Cl_2) $\nu(CO)$ = 2005,1884,1823; 1H -NMR ($CDCl_3$) δ =8.12 (d, 1H, J_{3-4} = 8.1 Hz, J_{3-5} <1.0 Hz, H-3), δ =7.95 (t, 1H, J_{4-5} = 7.5 Hz, H-4), δ =8.04 (d, 1H, H-5), δ =8.19(dd, 1H, H-3'), δ =7.99 (dt, 1H, $J_{4'-3}$ =7.5 Hz, H-4'), δ =7.42 (ddd, 1H, $J_{5'-4}$ =5.7 Hz, $J_{5'-3}$ =1.8 Hz, H-5'), δ =9.25 (dd, 1H, J_{6-5} =5.6 Hz, $J_{6'-4}$ <1.0 Hz, H-6'), δ = 5.01 (t, 2H, $J_{\alpha-\beta}$ =0.006 Hz, α - C_5H_5), δ = 4.60 (t, 2H, β - C_5H_5), δ = 4.15 (s, 5H, unsub- C_5H_5); ^{13}C -NMR ($CDCl_3$) δ =216.44 (1C, CO(2)), δ =212.08 (1C, CO(3)), δ =202.77 (2C, CO(1)), δ =164.49 (1C, C-6), δ =157.52 (1C, C-2), δ = 155.95 (1C, C-2'), δ =153.08 (1C, C-6'), δ =137.47 (1C, C-4), δ = 135.94 (1C, C-4'), δ =129.20 (1C-C-5), δ =125.58(1C, C-3), δ = 123.30 (1C, C-3'), δ =120.10 (1C, C-5'), δ =88.80 (1C, *i*- C_5H_5), δ =71.50 (2C, β - C_5H_5), δ = 69.90 (2C, α - C_5H_5), δ =70.47 (5C, unsub- C_5H_5); UV-VIS(CH_2Cl_2) $\lambda(CT)$ = 230 nm, 250 nm, $\lambda(d-d\text{-Fe(II)})$ =372 nm, 468 nm; $\lambda(d-d\text{-W(0)})$ =308 nm; CV(CH_2Cl_2) rev. red.(bpy)= -1.44, rev. ox(bpy)= -1.63, irrev. ox. pot($W \rightarrow W^+$)= 0.519, irrev. ox. pot($W^+ \rightarrow W^{+2}$)= 0.716, rev ox. Pot(fc)= 0.817, rev red. Pot(fc)=0.667, MS m/z = 636 (M^+), 605.9 ($M^+ - CO$), 577.9 ($M^+ - 2CO$), 549.9 ($M^+ - 3CO$), 521.9 ($M^+ - 4CO$).

3.3.4. Synthesis of Cr(CO)₄(fcbpy)

103 mg Cr(CO)₆ was dissolved in 150 mL THF and then irradiated for approximately one hour until the 80% of the starting complex turns into Cr(CO)₅(THF). The course of the reaction was followed by taking IR spectrum of the solution for every 20 minutes. Then the irradiation was stopped and 160 mg 6-ferrocenyl-2,2'-bipyridine was added. The solution was allowed to stir for ten days at room temperature. The solvent was evaporated under vacuum and IR spectrum was taken in CH₂Cl₂. IR(CH₂Cl₂) $\nu(\text{CO}) = 2006 \text{ cm}^{-1}$, 1980 cm^{-1} , 1894 cm^{-1} , 1829 cm^{-1} . The IR data indicates the formation of a complex containing the Cr(CO)₄- moiety. However, this complex could not be isolated from the solution.

CHAPTER 4

4. RESULTS AND DISCUSSION

4.1. Synthesis of 6-ferrocenyl-2,2'-bipyridine

In synthesis of ferrocenyl derivatives of dipyrindine, there are several strategies available which involves the reaction of ferrocenylmagnesium bromide⁵⁰ or ferrocenyl zincchloride^{51,52} with a halopyridine which is catalyzed by copper, nickel or palladium. Although reasonable yields of ferrocenyl substituted pyridines are expected from these reactions, they require the preparation of either haloferrocenes and/or halodipyrindines which add unnecessary synthetic steps.

The direct reaction of lithioferrocenes with the appropriate heteroaromatic compound yields much more lower product when compared to the other reactions, however, the synthesis involve essentially one step reaction. In both cases, a mixture of products was obtained but the one shown to predominate by the tlc analysis of the crude organic phase was obtained in a pure form by column chromatography. For this reason, the synthesis of 6-ferrocenyl-2,2'-bipyridine was performed by the direct reaction by lithioferrocene with 2,2'-bipyridine. The average yield of this reaction was found as 37% (range 30-40%).⁴⁸ The reaction is shown in Figure 4.1.

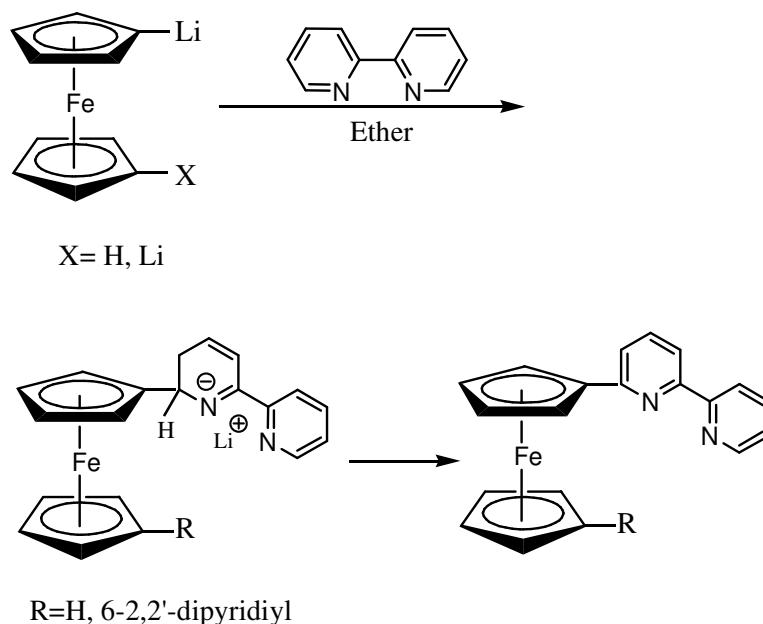


Figure 4.1. The reaction of lithioferrocene with 2,2'-bipyridine

The major product in the reaction is derived from the attack at 2-position which gives rise to favorable resonance intermediate where the negative charge may be localized on the nitrogen atom.⁵³ In all reactions reported to date where the ferrocenyl anion is a nucleophile towards bipyridines attack at a position ortho to the nitrogen predominates, resulting the compounds such as 6-ferrocenyl-2,2'-bipyridine.⁵⁴

The orange colored crystals of fcbpy were characterized by using NMR and UV-VIS spectroscopy techniques. The formation of the ligand was shown clearly by the use of ^1H , ^{13}C and HMQC NMR spectra as follows:

When the suggested structure of the ligand, 6-ferrocenyl-2,2'-bipyridine, is examined, it is seen that there are 10 different hydrogens and 14 different carbon atoms. Accordingly, one expects 10 signals in the ^1H -NMR and 14 signals in the ^{13}C -NMR spectrum.

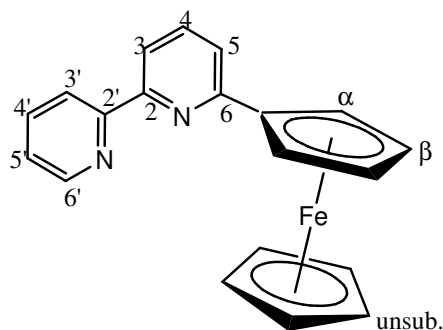


Figure 4.2. The suggested structure of 6-ferrocenyl-2,2'-bipyridine

According to the $^1\text{H-NMR}$ spectrum (Figure 4.3), H-6', which is in ortho position to nitrogen atom, is the most deshielded hydrogen atom in the dipyriddy moiety giving a doublet at 8.62 ppm. The signal appears in lower field because of the strong electron withdrawing effect of the nitrogen atom. H-3' resonates at 8.51 ppm giving a doublet. A doublet at 8.14 ppm, a doublet of triplets at 7.78 ppm, a triplet at 7.65 ppm, a doublet at 7.36 ppm and a doublet of doublet of doublet at 7.24 ppm belong to H-3, H-4', H-4, H-5 and H-5', respectively. Because of the anisotropic effect of the rings of the bipyridyl moiety, H-3' and H-3 protons resonate at lower field with respect to other hydrogen atoms. From the $^1\text{H-NMR}$ spectrum, it is also observed that the hydrogen atoms of the ferrocenyl moiety give signals in the range of 4-5 ppm. The unsubstituted cyclopentadienyl (Cp) ring gives a singlet for its 5 equivalent hydrogens at 3.98 ppm. The α -hydrogen atom of the substituted Cp ring gives a triplet at 4.96 ppm, and β -hydrogen also gives a triplet at 4.35 ppm. The most deshielded proton of the ferrocenyl moiety is the one in the α -position due to its closeness to the electron withdrawing bipyridine moiety. The intensity ratio of signals belong to α -, β - and unsubstituted hydrogen atoms is 2:2:5 respectively. The couplings of hydrogen atoms of 6-ferrocenyl-2,2'-bipyridine are as follows: $J(5'-6') = 4.7$ Hz, $J(6'-4') = 1.7$ Hz, $J(5'-4') = 7.8$ Hz, $J(5'-3') = 1.1$ Hz, $J(3-4) = 7.7$ Hz, $J(4-5) = 7.8$ Hz, $J(3-5) = 0.7$ Hz, $J(\alpha-\beta) = 1.8$, $J(6'-3') \sim 0$,

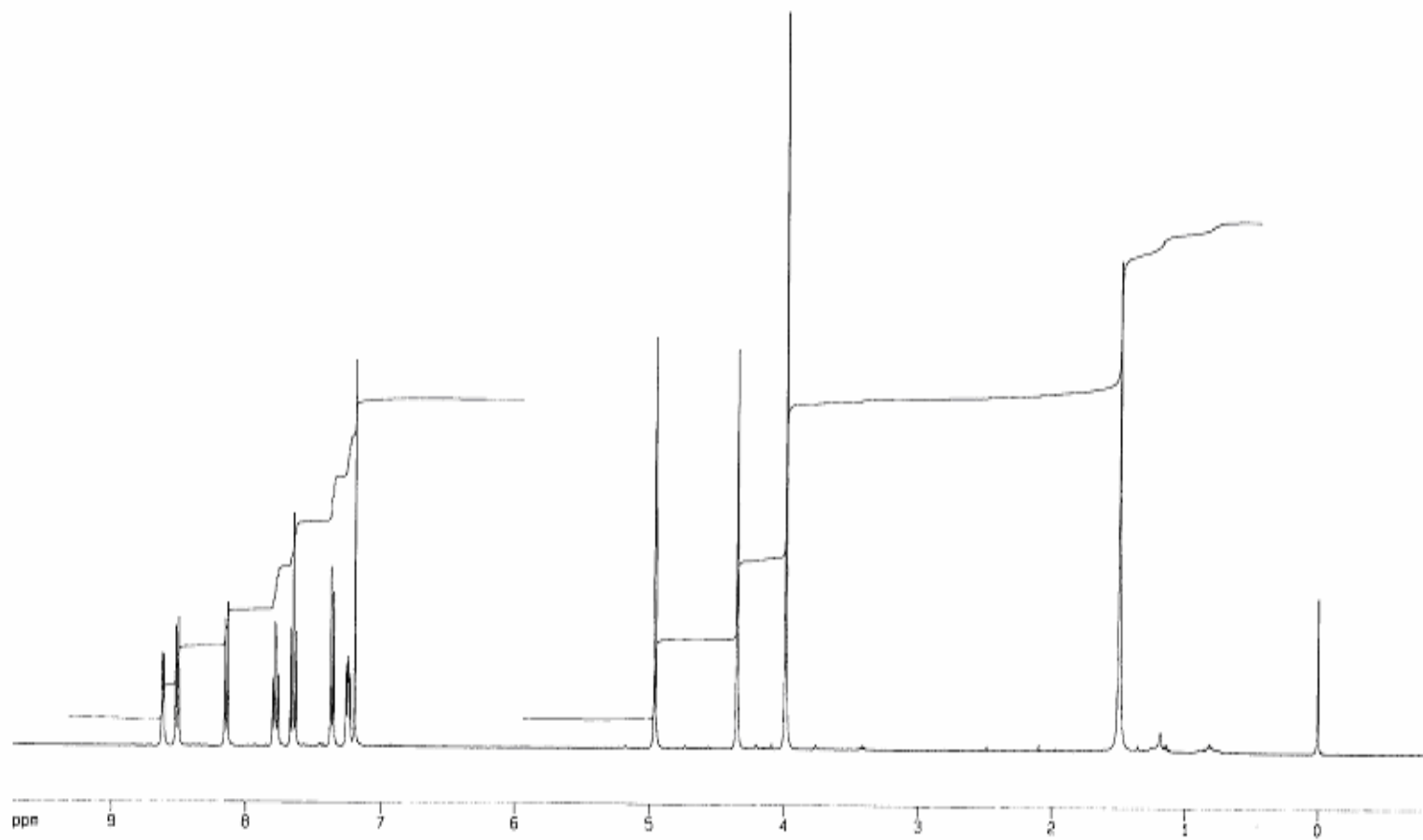


Figure 4.3. $^1\text{H-NMR}$ Spectrum of 6-ferrocenyl-2,2'-bipyridine

In the ^{13}C -NMR spectrum (Figure 4.4), 14 signals are observed as expected from the suggested structure. The carbon atoms of the ferrocenyl moiety resonate in the range between 60-90 ppm whereas carbon atoms of the aromatic bipyridine moiety, give signals in the range of 110-160 ppm. The most deshielded carbon atoms C-6, C-2', C-2 resonate at 157.45 ppm, 155.60 ppm and 154.27 ppm. It is not possible to make the exact assignments to C-2', C-2 carbon atoms due to their close resonances and structural positions but C-6 can be assigned as the most deshielded one with its signal at 157.45 due to the closeness to the ferrocenyl group. C-6' resonates at 147.97 ppm since it is in the ortho position to nitrogen atom. C-4 and C-4' resonates at 135.78 and 135.76 ppm, respectively. Although these peaks are very close to each other, the use of HMQC spectrum (Figure 4.5) enables us to make the exact assignments of these two signals to the carbon atoms C-4 and C-4', as the corresponding ^1H -NMR signals are unambiguously assigned as the bases of their multiplicities. The signals at 122.52, 120.18, 119.01 and 116.66 belong to C-5', C-3', C-5 and C-3, respectively. The assignment of these peaks is also made by using the HMQC spectrum together with the ^1H -NMR spectrum. The ipso carbon of the ferrocenyl group gives a signal at 83.13 ppm as the most deshielded atom in the ferrocenyl moiety due to its closeness to electron withdrawing group. Five unsubstituted carbon atoms in Cp ring resonate at 68.58 ppm. The α - and β - carbon atoms of the substituted Cp ring give signals at 66.44 and 68.78 ppm, respectively.

Hydrogen and carbon atoms of the unsubstituted cyclopentadienyl ring are actually not equivalent but they are equalized by the free rotation through Fe-Cp bond axis. This fact is observed from the ^1H - and ^{13}C -NMR spectra of ferrocene. It has only one singlet at 4.07 ppm in the ^1H -NMR spectrum and a signal at 68.3 ppm in the ^{13}C -NMR spectrum taken in d-chloroform.¹⁹

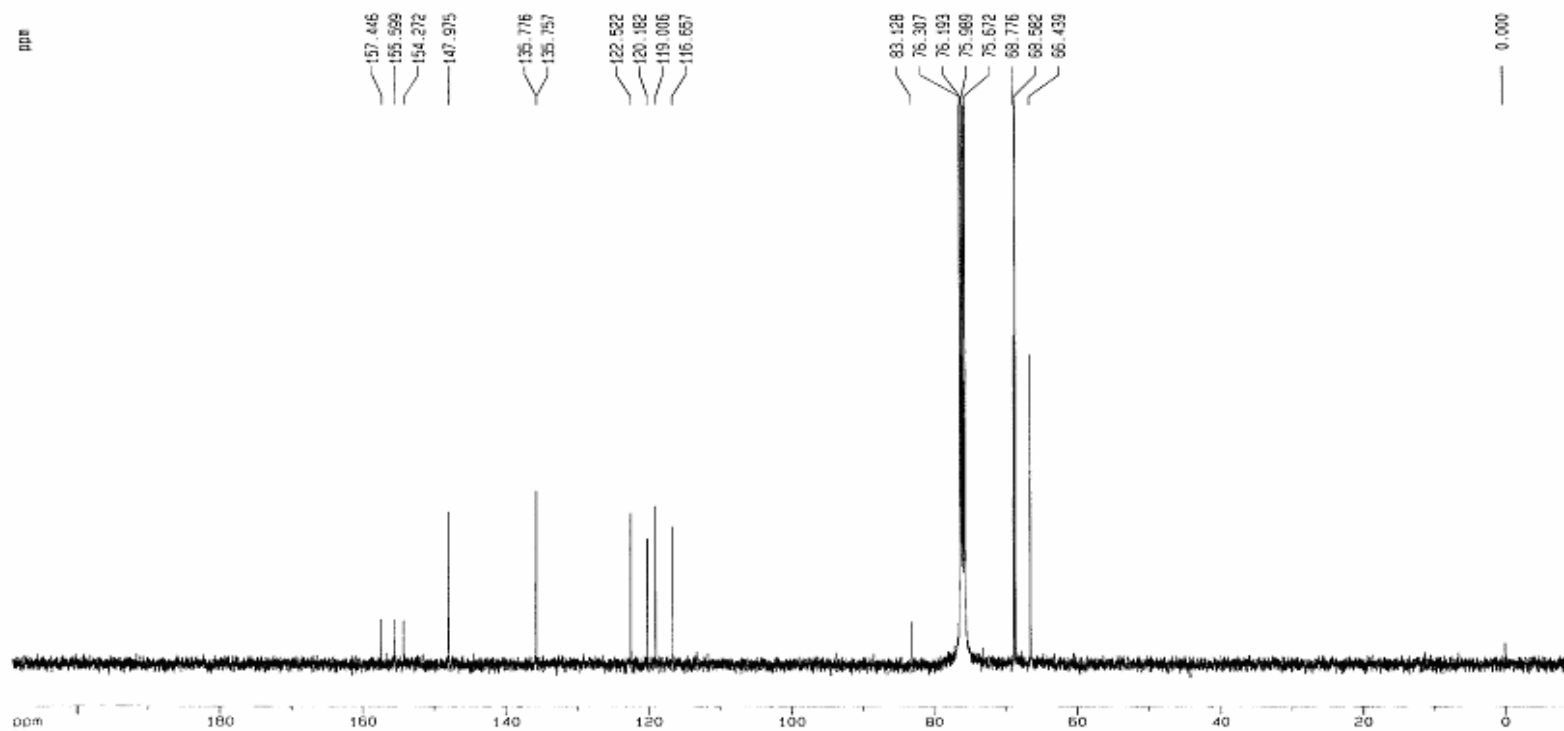


Figure 4.4. ^{13}C -NMR Spectrum of 6-ferrocenyl-2,2'-bipyridine.

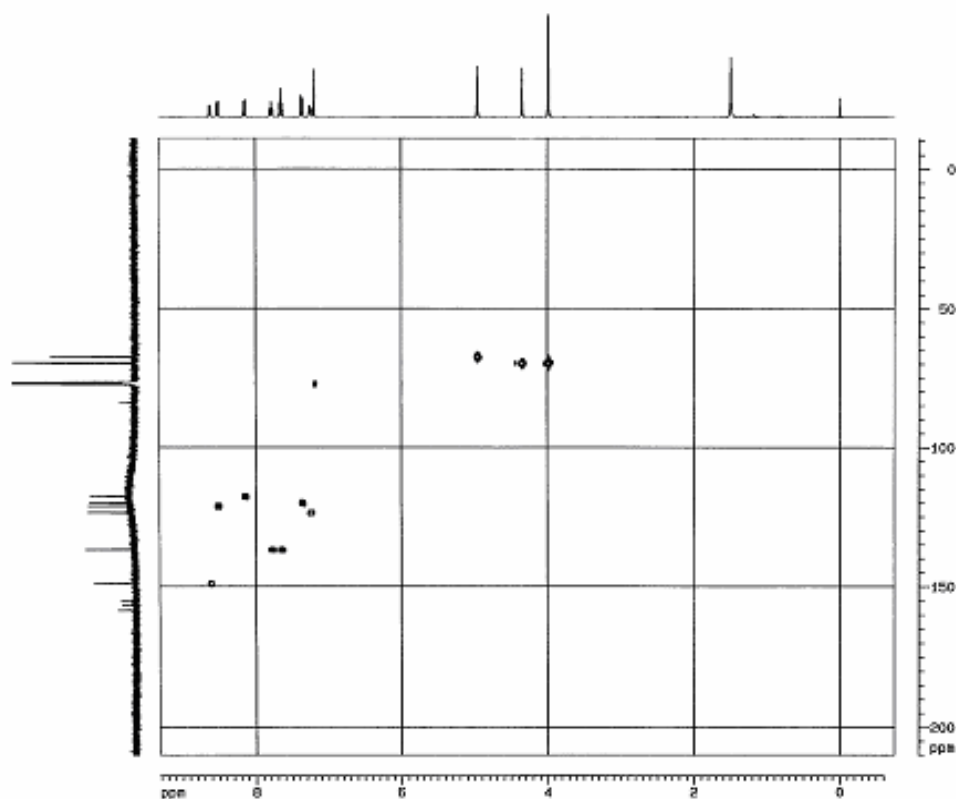


Figure 4.5. HMQC spectrum of 6-ferrocenyl-2,2'-bipyridine.

NMR spectra of the fcbpy molecules indicate that ferrocenyl group binds the bipyridine in ortho position through one of its cyclopentadienyl rings confirming the suggested formula of the fcbpy. When the ^1H - and ^{13}C -NMR spectra of 2,2'-bipyridine molecule compared with those of fcbpy, it is easily recognized that pyridyl protons and carbons are shielded by ferrocenyl ring, while the α - and β - hydrogen atoms experience some deshielding due to the electron withdrawing bipyridiyl substituent. The chemical shift differences of protons and carbons in comparison to unsubstituted dipyridyl and ferrocene are given in Table 4.1 and Table 4.2.

Table 4.1. The chemical shift differences of protons of fcbpy with respect to free ferrocene and unsubstituted bipyridine.

H	$\Delta\delta$ (H), ppm
3	0.28
4	0.19
5	-0.13
3'	-0.09
4'	0.06
5'	0.00
6'	0.08
α	-0.89
β	-0.28

Table 4.2. The chemical shift differences of carbon atoms of fcbpy with respect to free ferrocene and unsubstituted bipyridine

C	$\Delta\delta$ (C), ppm
2	0.57
3	4.44
4	1.12
5	4.68
6	1.19
2'	1.90
3'	0.9
4'	1.14
5'	1.17
6'	-8.27
α	1.86
β	-0.47

By using HMQC spectrum (Figure 4.5), one can see the correlation between carbon and hydrogen atoms which are directly bonded to each other. According to the HMQC spectrum of the ligand, the signals at 157.45, 155.60, 154.27 and 84.14 ppm are due to the carbon atoms which do not have any hydrogen attached. Therefore, these signals are readily assigned to C-6, C-2', C-2 and ipso carbon. The other hydrogen-carbon correlations provide useful information for the assignments of the ^{13}C -NMR signals as mentioned before.

The UV-VIS spectrum of the ligand, 6-ferrocenyl-2,2'-bipyridine, given in Figure 4.6 shows four absorption bands at 234, 286, 354 and 460 nm. The absorption bands of the fcbpy ligand were compared to those of free ferrocene described in literature.⁵⁵ Free ferrocene has three charge transfer bands at 265, 239 and 200 nm and two d-d transitions at 458 and 324 nm. It is also known from strong field theory that, free or substituted ferrocene has three spin allowed transitions. According to these information, the bands at 234 and 286nm are assigned as charge transfer transitions whereas the ones observed at 354 and 460 nm are assigned as d-d transitions ($\epsilon_{234\text{nm}}= 3.3 \times 10^4$, $\epsilon_{286\text{nm}}= 2.2 \times 10^4$, $\epsilon_{354\text{nm}}= 6.3 \times 10^3$, $\epsilon_{460\text{nm}}= 2.9 \times 10^3 \text{ Lmol}^{-1}\text{cm}^{-1}$)

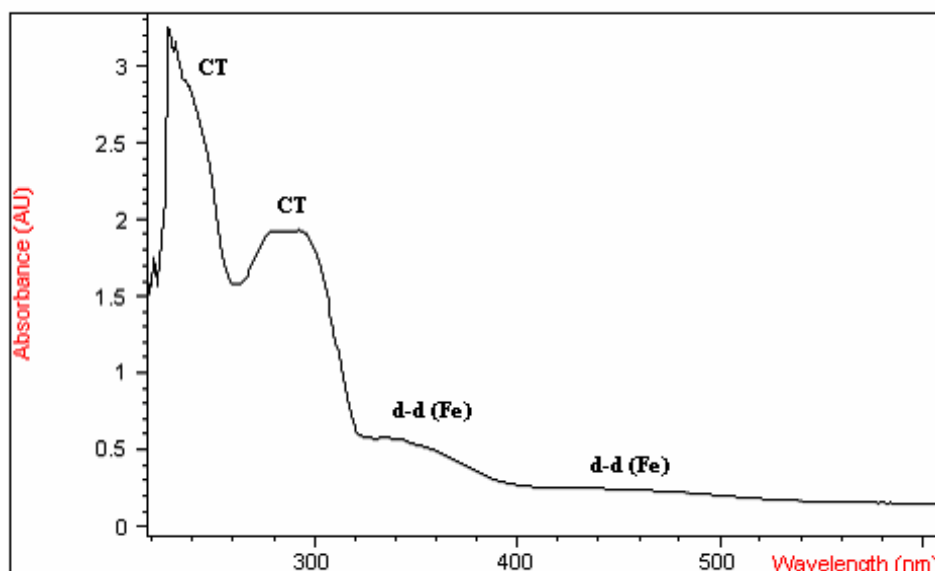


Figure 4.6. The UV-VIS spectrum of 6-ferrocenyl-2,2'-bipyridine in CH_2Cl_2 , taken at room temperature.

Cyclic voltammogram of ligand exhibits an irreversible reduction peak at -1.250 V which belongs to bipyridine⁵⁶ and a reversible oxidation peak at 0.710V which shows the electron transfer of ferrocene (Figure 4.7).

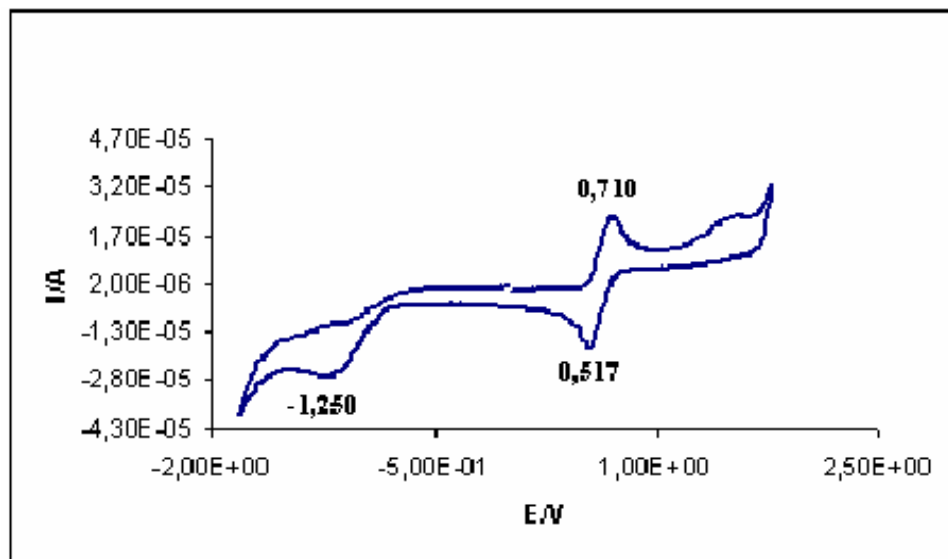


Figure 4.7. Cyclic voltammogram of 6-ferrocenyl-2,2'-bipyridine in CH_2Cl_2 , taken at room temperature. Electrolyte: tetrabutylammonium tetrafluoroborate. Reference electrode: SCE

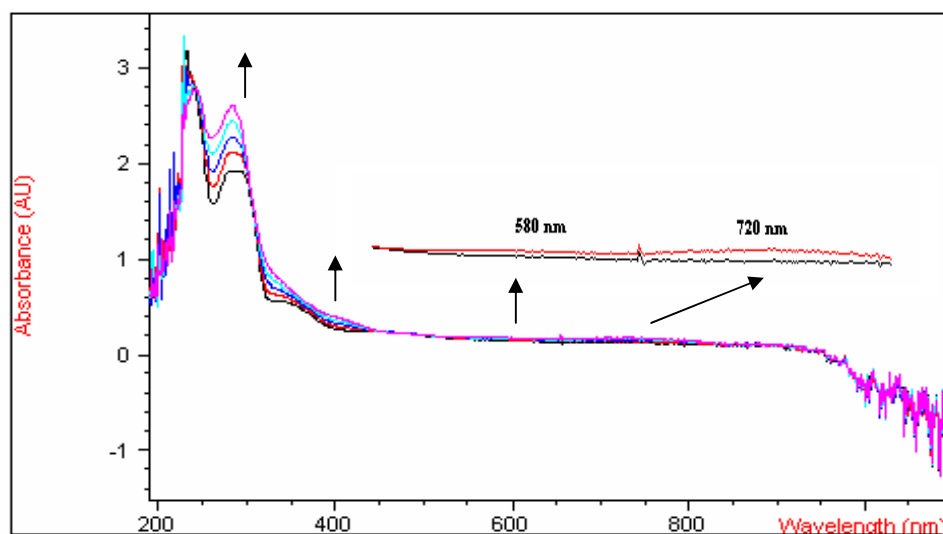


Figure 4.8. The UV-VIS electronic absorption spectra of 6-ferrocenyl-2,2'-bipyridine recorded during its electrolytic oxidation in CH_2Cl_2 solution. Electrolyte; tetrabutylammonium tetrafluoroborate.

The UV-VIS absorption spectra of 6-ferrocenyl-2,2'-bipyridine during its electrolytic oxidation are shown in Figure 4.8. The electrolysis was carried out at the oxidation peak potential of 0.710 V as observed in the CV of the ligand. Ag wire was used as the reference electrode. As the oxidation proceeds, the band at 286 nm started to increase with a shift to lower energy. There is also an increase in the intensities of the bands at 354 nm and 460 nm. At the end of the electrolysis the formation of two bands were observed at 580 nm and 720 nm which indicates the oxidation of the ligand.

4.2. Synthesis of Tetracarbonyl(6-ferrocenyl-2,2'-bipyridine)tungsten(0)

The synthesis of tetracarbonyl(6-ferrocenyl-2,2'-bipyridine)tungsten(0) was carried out by the substitution reaction of $W(CO)_5(\eta^2\text{-btmse})$ complex with 6-ferrocenyl-2,2'-bipyridine in CH_2Cl_2 at room temperature. The reason of choosing $W(CO)_5(\eta^2\text{-btmse})$ as the starting complex is that it has been shown to be very labile towards the substitution of btmse and/or CO ligand in the presence of a potential ligand.⁴⁶ Moreover, btmse provides stability for $M(CO)_5$ -moiety, just enough to be isolated. Thus, the $W(CO)_5(\eta^2\text{-btmse})$ complex could be isolated as pure crystalline solid.

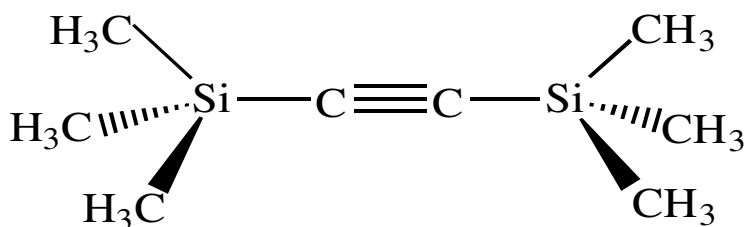
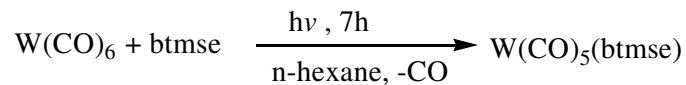
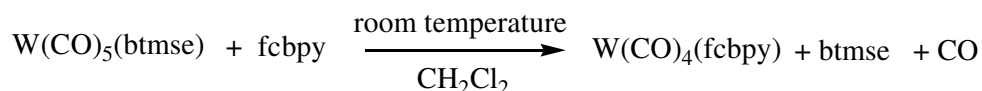


Figure 4.9. Bis-(trimethyl)silylethyne (btmse)

First, $W(CO)_5(\eta^2\text{-btmse})$ was prepared by irradiating $W(CO)_6$ with btmse in n-hexane solution for 7 hours.



Then, the thermal substitution reaction of $\text{W(CO)}_5(\eta^2\text{-btmse})$ with 6-ferrocenyl-2,2'-bipyridine was carried out at room temperature by stirring for 45 hours.



The reaction was followed by taking the IR spectra throughout the experiment. The starting complex, $\text{W(CO)}_5(\eta^2\text{-btmse})$ has local C_{2v} symmetry with five $\nu(\text{CO})$ vibrations of $3A_1$, B_1 and B_2 . However, one of the A_1 mode should be intrinsically weak in intensity and may remain unobserved or barely observable.⁴⁶ As a result, the IR spectrum shows five $\nu(\text{CO})$ absorption bands at 2079, 1986, 1960, 1955 and 1939 along with one absorption band at 1905 cm^{-1} for the $\text{C}\equiv\text{C}$ stretching. The absorption bands and their vibrational modes are given in Table 4.3.

Table 4.3. The vibrational modes and IR bands of $\text{W(CO)}_5(\eta^2\text{-btmse})$.

Vibrational Modes	IR Bands, cm^{-1}
A_1^1	2079
A_1^2	1986
B_1	1960
B_2	1955
A_1^3	1939
$\text{C}\equiv\text{C}$	1905

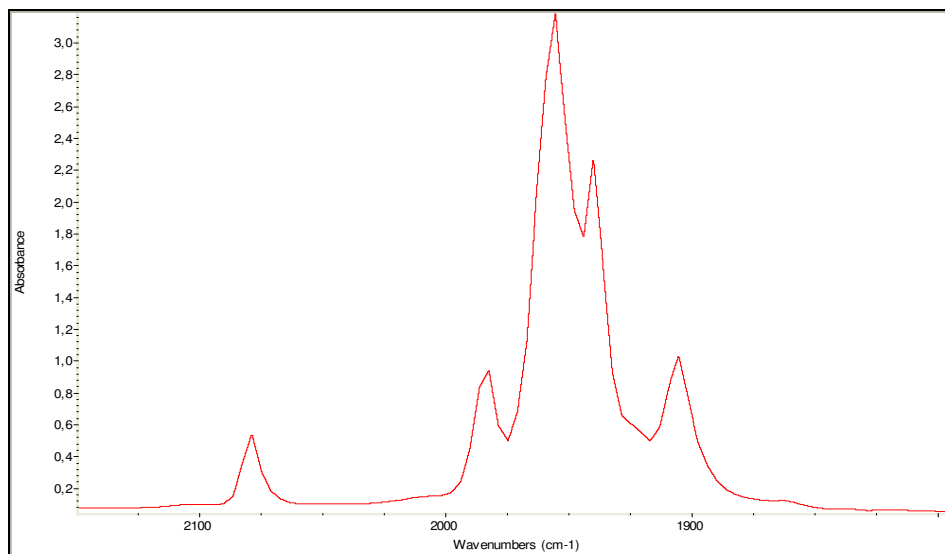


Figure 4.10. The IR Spectrum $W(CO)_5(\eta^2\text{-btmse})$ in CH_2Cl_2 taken at room temperature

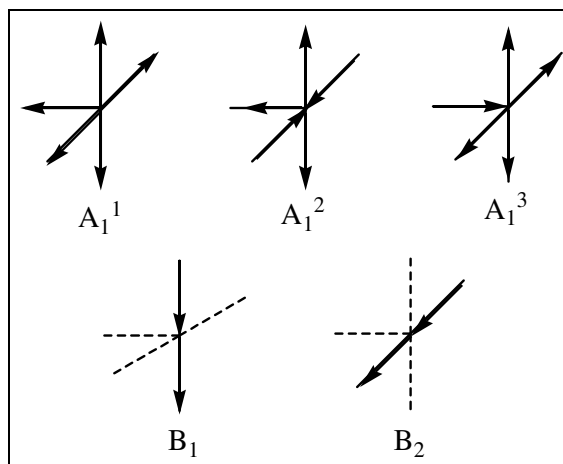


Figure 4.11. Symmetry coordinates for the CO stretching vibrational modes in $W(CO)_5(\eta^2\text{-btmse})$.

The formation of tetracarbonyl(6-ferrocenyl-2,2'-bipyridine)tungsten(0) complex begins one hour after starting the reaction. Three absorption bands at 2005, 1884 and 1823 cm^{-1} appear and increase in intensity as the reaction proceeds indicating the presence of a tetracarbonyl complex, while, the absorption bands of the starting complex loose intensity. It is also observed that, an additional absorption band at 1975 cm^{-1} grows in due to the formation of $\text{W}(\text{CO})_6$. Figure 4.12 shows the formation of new bands of $\text{W}(\text{CO})_4(\text{fcbpy})$. The color of the reaction solution turns from orange to dark red as absorption bands of the desired complex start to appear.

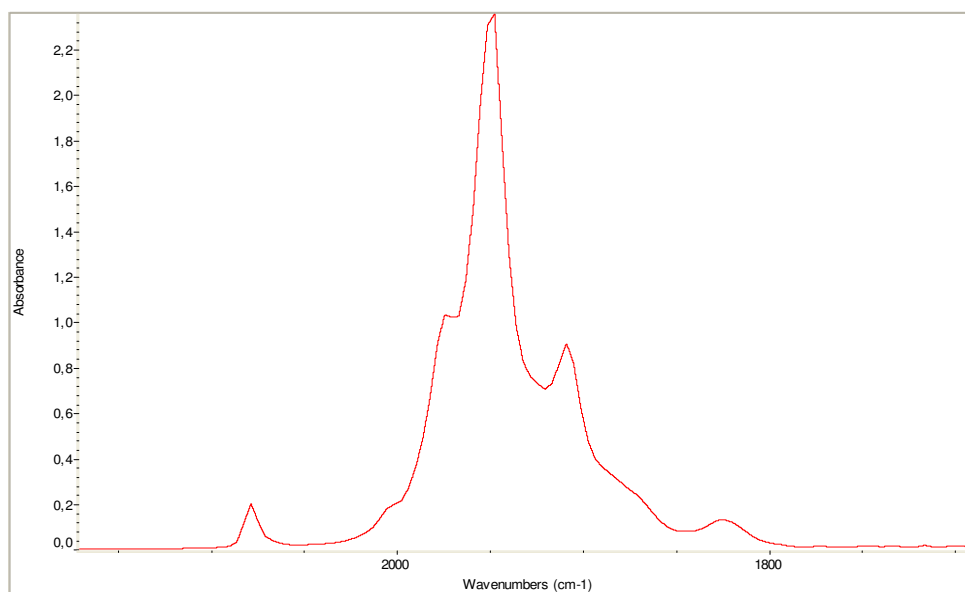


Figure 4.12. The FTIR spectrum taken 1 hour after the beginning of the thermal substitution of $\text{W}(\text{CO})_5(\eta^2\text{-btmse})$ with fcbpy in CH_2Cl_2 taken at room temperature.

After 45 hours stirring, the reaction is complete. However there is also a large amount of $\text{W}(\text{CO})_6$ which can be recognized from the absorption band at 1975 cm^{-1} . In order to remove $\text{W}(\text{CO})_6$, the reaction solution was evaporated under vacuum and the remaining solid was allowed to cool down to -40°C for

crystallization, whereby some of the free ligand precipitated. Column chromatography was performed under nitrogen atmosphere by using a special glassware. The unreacted ligand, fcbpy was eluted by using n-hexane and THF. Then, acetonitrile was used as eluent in order to collect the complex, $W(CO)_4(fcbpy)$, portion. The solvent was removed under vacuum. The FTIR spectrum of the pure complex is given in Figure 4.13.

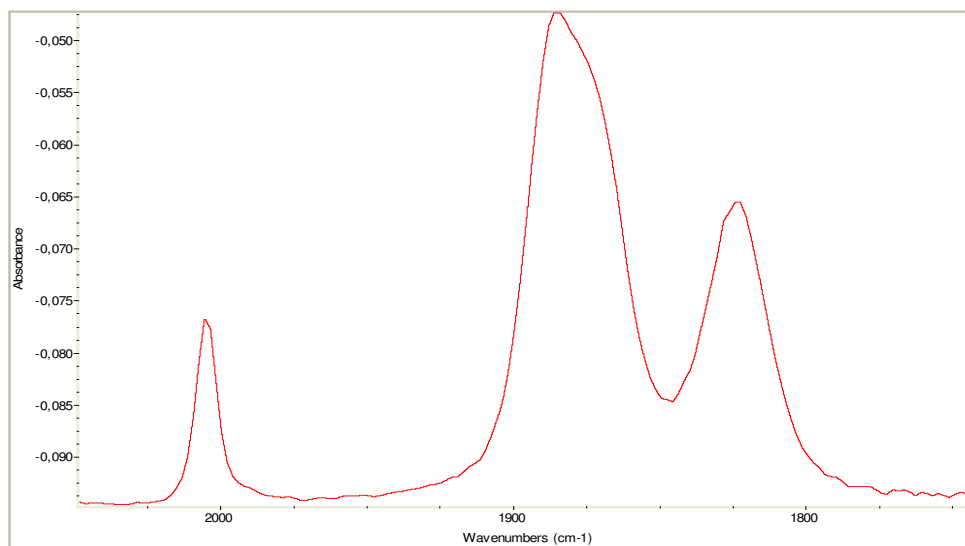


Figure 4.13. The FTIR spectrum of $W(CO)_4(fcbpy)$.

Four absorption bands are observed at 2005, 1884, 1870 and 1823 cm^{-1} for the CO stretching in $W(CO)_4(fcbpy)$ indicating a local C_{2v} symmetry for the $W(CO)_4$ moiety in the complex. Thus, the complex molecule has four vibrational modes of $2A_1 + B_1 + B_2$ for the CO stretching. The symmetry coordinates for the CO stretching vibrational modes in the $W(CO)_4(fcbpy)$ are given in Figure 4.14. The absorption bands and their vibrational modes are given in Table 4.4.

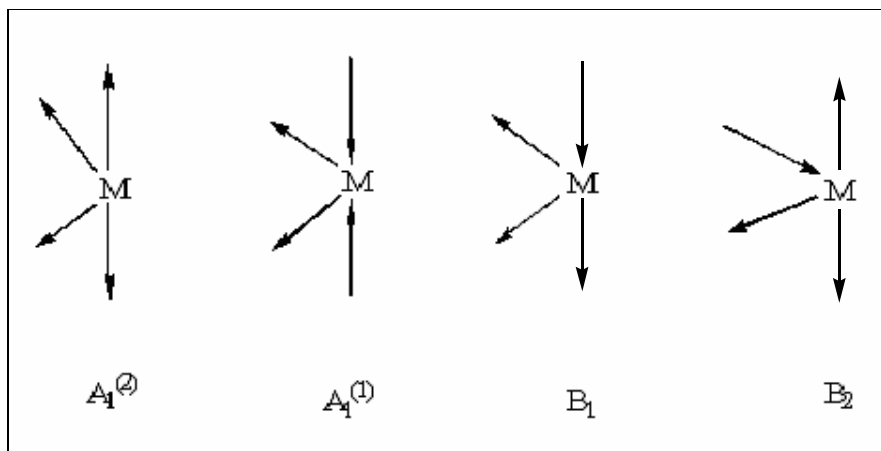


Figure 4.14. The symmetry coordinates for the CO stretching vibrational modes in the $W(CO)_4(fcbpy)$

Table 4.4. The absorption bands and their vibrational modes of $W(CO)_4(fcbpy)$ in CH_2Cl_2 .

Vibrational Modes	IR Bands, cm^{-1}
A_1^2	2005
B_1	1884
A_1^1	1870
B_2	1823

The suggested structure of the complex, $W(CO)_4(fcbpy)$, exhibits 10 different hydrogen atoms and 17 different carbon atoms.

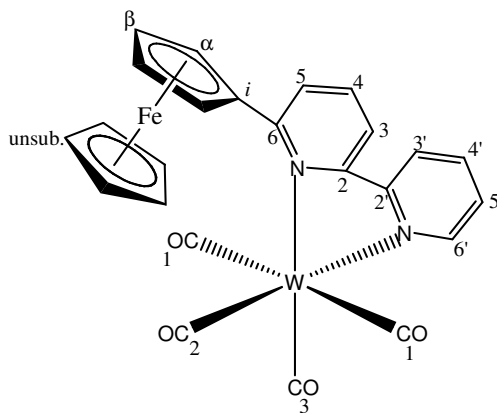


Figure 4.15. $W(CO)_4(fcbpy)$ structure

1H -NMR spectrum of the $W(CO)_4(fcbpy)$ shows similar pattern to that of the free fcbpy molecule. However, all peaks are shifted to lower magnetic field upon coordination due to the electron-withdrawing effect of $W(CO)_4$ moiety. The 1H -NMR spectrum of the complex gives two triplets for the substituted cyclopentadienyl ring hydrogen atoms and one singlet for the five hydrogen atoms of the unsubstituted cyclopentadienyl ring. The α and β hydrogen atoms on the substituted ring resonate at 5.01 and 4.60 ppm, respectively. The singlet at 4.15 ppm is due to the five equivalent hydrogens. The relative signal ratio of the protons on the cyclopentadienyl rings is 2:2:5. In addition, one observes a doublet at 9.25 ppm for H-6' as the most deshielded hydrogen atom, a doublet of doublet at 8.19 ppm for H-3', a doublet at 8.12 ppm for H-3, a doublet of triplets at 7.99 ppm for H-4', a triplet at 7.95 ppm for H-4, a doublet at 8.04 ppm for H-5 and a doublet of doublet of doublets at 7.42 ppm for H-5'. The most shielded hydrogen atom is H-5' as expected. The region between 7.92 ppm- 8.03 ppm which involves the signals of H-4, H-4' and H-5' is very complex for making the correct assignments since it turns to be a second order nmr spectrum rather than a first order. As a result, intensity distribution of the signals changes and to separate the signals from each other gets harder. The coupling constants of hydrogen atoms are as follows: $J(6'-5')=5.6$ Hz, $J(6'-4')<1.0$ Hz, $J(5'-4')= 5.7$ Hz, $J(5'-3')=1.8$ Hz, $J(4'-3')= 7.5$ Hz, $J(3-4)= 8.1$ Hz, $J(4-5)= 7.5$ Hz, $J(3-5)<1.0$ Hz.

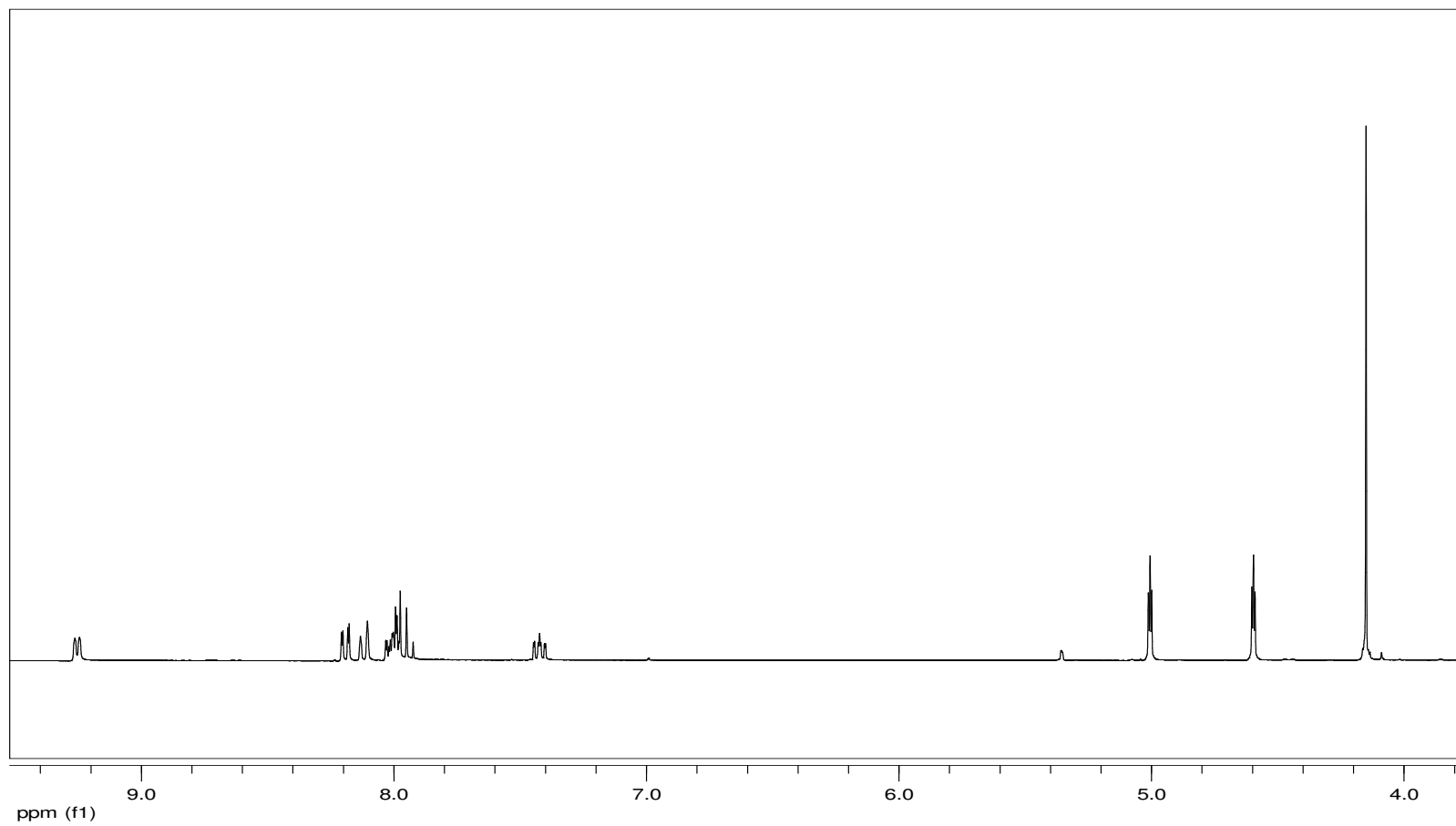


Figure 4.16. $^1\text{H-NMR}$ spectrum of $\text{W}(\text{CO})_4(\text{fcbpy})$ in CD_2Cl_2

¹³C-NMR spectrum shows three signals in the range of 200-220 ppm for the carbonyl carbon atoms. The ones at 216.44 and 212.48 ppm are belong to carbonyls, CO(3) and CO(2), trans to one nitrogen atom of the fcbpy ligand and the one at 202.77 ppm is for two equivalent CO ligands which are trans to each other. The ratio of the signals is 1:1:2 which indicates the presence of 4 carbonyls, two of which are equal. The deshielding of the carbonyl carbons which are trans to imines denotes the lower π -accepting and higher σ -donating abilities of fcbpy compared to carbon monoxide.²⁶ The other carbon atoms on the bipyridine moiety show a lower field shift upon coordination to tungsten center. As expected from the closeness of the carbon atoms to the coordination site, the highest coordination shift value belongs to the imine carbon atoms C-6, C-6', C-2 and C-2'. These carbon atoms in the coordinated fcbpy ligand resonate at 164.49, 153.08, 157.52 and 155.95 ppm, respectively. In addition, the signals at 137.47, 135.94, 129.20, 125.58, 123.30, 120.10 belong to C-4, C-4', C-5, C-3, C-3' and C-5' carbon atoms, respectively. The ipso, α and β - carbons of ferrocene moiety give signals at 88.80, 69.90 and 71.50, respectively. The five carbon atoms of the unsubstituted Cp ring resonate at 70.47 ppm. The chemical shift differences of protons and carbons of the complex with respect to those of the free fcbpy molecule are given in Table 4.5 and Table 4.6. From Table 4.5, it is seen that H-3 and H-3' protons shift to higher field upon coordination to a metal center. In the free fcbpy molecule, the planes of the pyridyl rings are tilted with respect to each other, so that the H-3 and H-3' protons are in the deshielding cone of the neighboring aromatic ring. However, after the formation of the complex, these rings are forced to be coplanar by the chelation. As a result the deshielding of the protons due to the anisotropic effect of the aromatic ring currents is not observed in the case of complex.

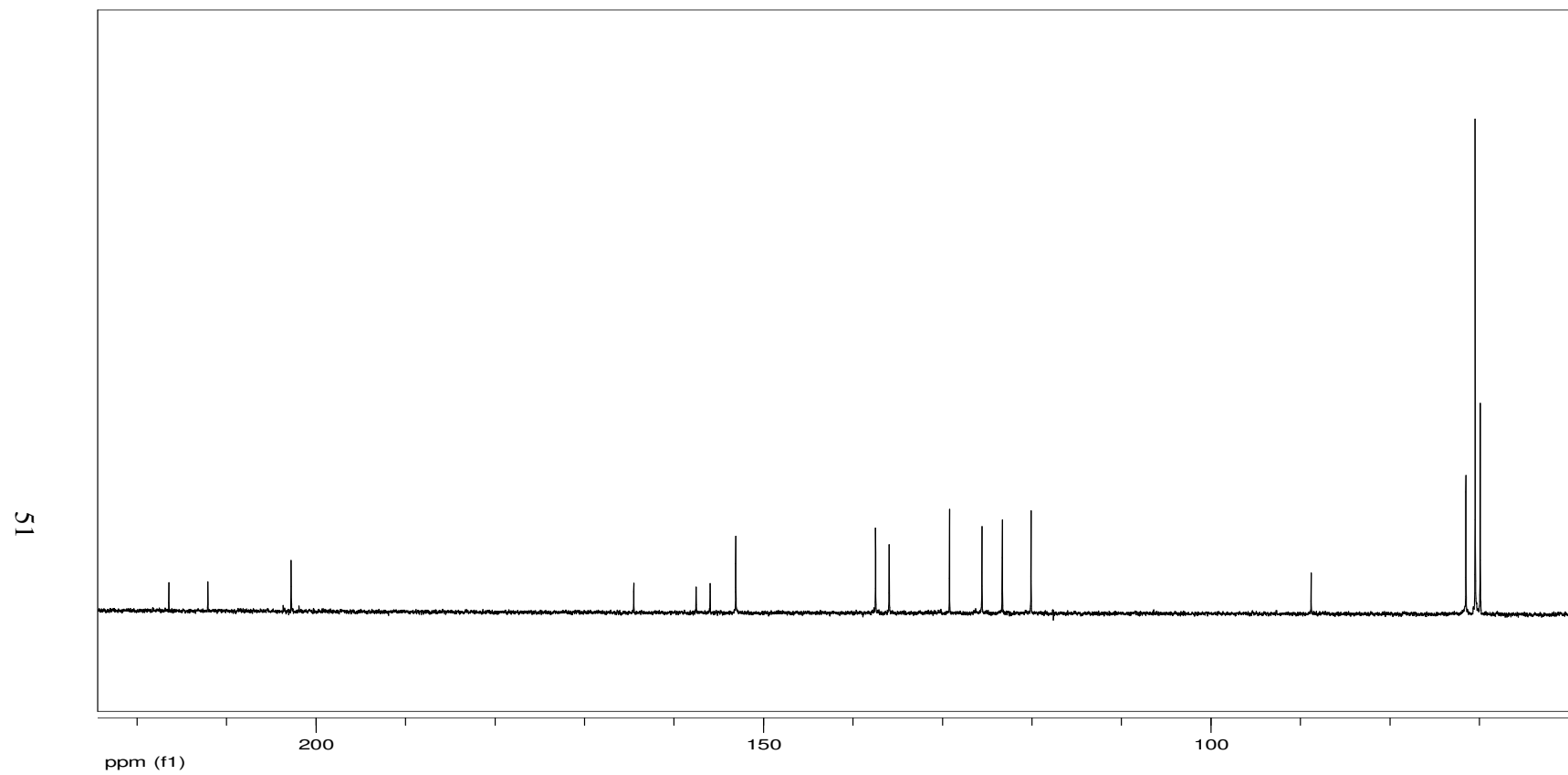


Figure 4.17 ^{13}C -NMR spectrum of $\text{W}(\text{CO})_4(\text{fcbpy})$ CD_2Cl_2

Table 4.5. ^1H - NMR chemical shifts (δ , ppm) of fcbpy and $\text{W}(\text{CO})_4(\text{fcbpy})$, and coordination shift values ($\Delta\delta$, ppm).

	δ (H-5)	δ (H-4)	δ (H-3)	δ (H-3')	δ (H-5')	δ (H-4')	δ (H-6')	δ (H- α)	δ (H- β)	δ (H- unsub.)
Fcbpy	7.36	7.65	8.14	8.51	7.24	7.78	8.62	4.96	4.35	3.98
$\text{W}(\text{CO})_4(\text{fcbpy})$	8.04	7.95	8.12	8.19	7.42	7.99	9.25	5.01	4.60	4.15
Coordination shift, $\Delta\delta$ (ppm)	-0.68	-0.3	0.02	0.32	-0.18	-0.21	-0.63	-0.05	-0.25	-0.17

Table 4.6. ^1H - NMR chemical shifts (δ , ppm) of fcbpy and $\text{W}(\text{CO})_4(\text{fcbpy})$, and coordination shift values ($\Delta\delta$, ppm).

	δ (C-5)	δ (C-4, C- 4')	δ (C-3)	δ (C-3')	δ (C-5')	δ (C-6')	δ (C- α)	δ (C- β)	δ (C- unsub)	δ (i)	δ (*C-6, C-2', C-2)
Fcbpy	119.01	135.76, 135.78	116.66	120.18	122.52	147.97	66.44	68.78	68.58	83.13	*157.45, 155.60, 154.27
$\text{W}(\text{CO})_4(\text{fcbpy})$	129.20	137.47, 135.94	125.58	123.30	120.10	153.08	69.90	71.50	70.47	88.80	*164.49 157.52 155.95
Coordination shift, $\Delta\delta$ (ppm)	-10.19	-1.71 -0.16	-8.92	-3.12	2.42	-5.11	-3.46	-2.72	-1.89	-5.67	*-7.04 -1.92 -1.68

Table 4.7 shows the elemental analysis results for the nitrogen, hydrogen and carbon atoms and their theoretical mass percentages in $W(CO)_4(fcbpy)$. The experimental and theoretical values are close to each other.

Table 4.7. Elemental analysis values and theoretical mass percentages of carbon, nitrogen and hydrogen atoms in $W(CO)_4(fcbpy)$

ATOM	EXPERIMENTAL %	THEORETICAL %
CARBON	44.3	45.3
HYDROGEN	2.83	2.54
NITROGEN	4.20	4.40

For further characterization of $W(CO)_4(fcbpy)$, fast atom bombardment mass spectroscopy (FAB) was used. The calculated molecular weight of the complex is 636 g/mol. The FAB-MS spectrum of the $W(CO)_4(fcbpy)$ complex given in Figure 4.18 shows the molecular peak with the unique isotope distribution. Figure 4.19 shows the simulated molecular peak for $W(CO)_4(fcbpy)$ which fits well with the experimental one in Figure 4.20.

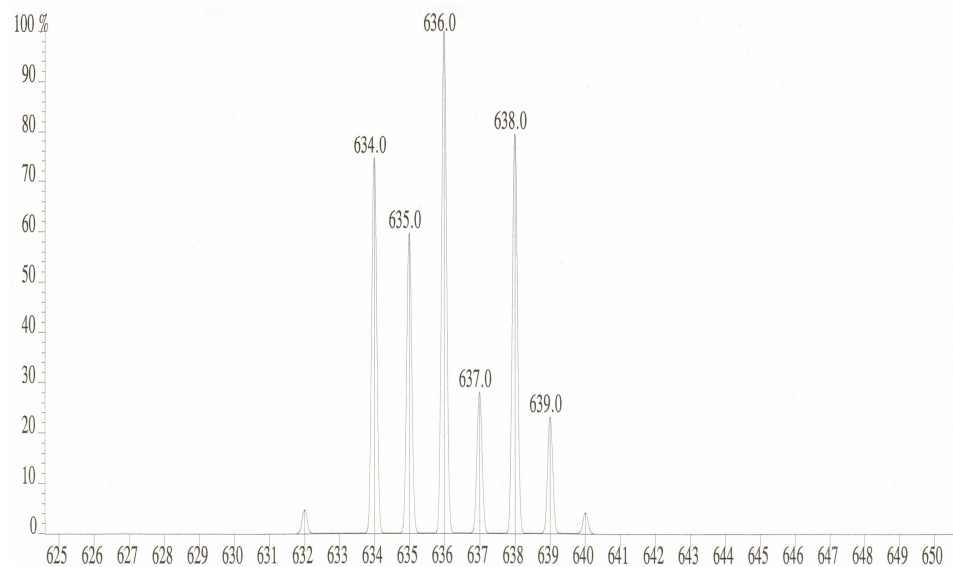


Figure 4.18. Molecular peak in the mass spectrum of $W(CO)_4(fcbpy)$

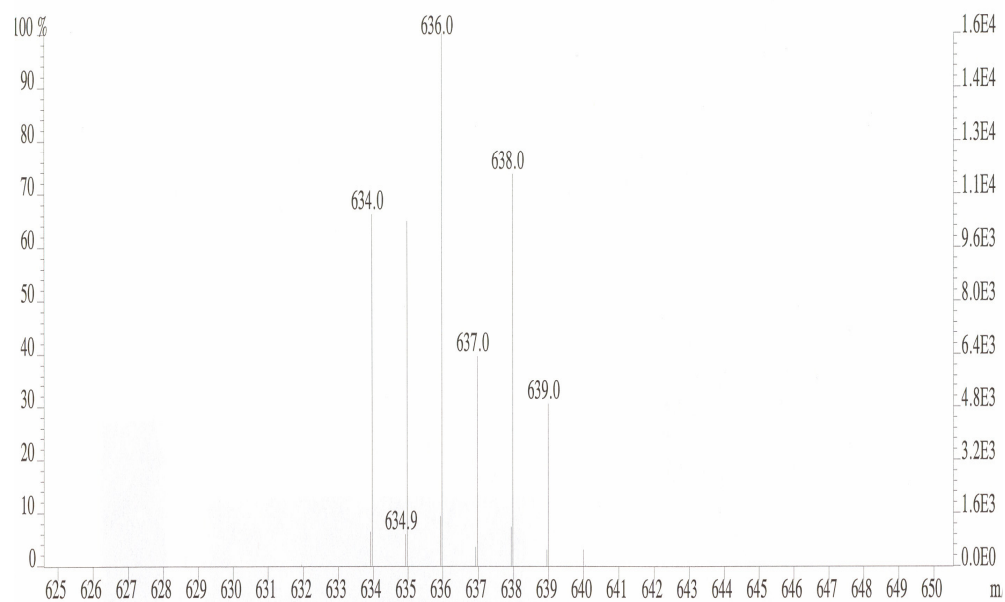


Figure 4.19. Calculated molecular peak of the complex, $W(CO)_4(fcbpy)$

The full FAB-MS spectrum given in Figure 4.20 shows the sequential detachment of four CO groups from the complex. Figure 4.20 exhibits the CO lost fragments at $m/z = 607.9$ ($M^+ - CO$), 579.9 ($M^+ - 2CO$), 551.9 ($M^+ - 3CO$), 523.9 ($M^+ - 4CO$)].

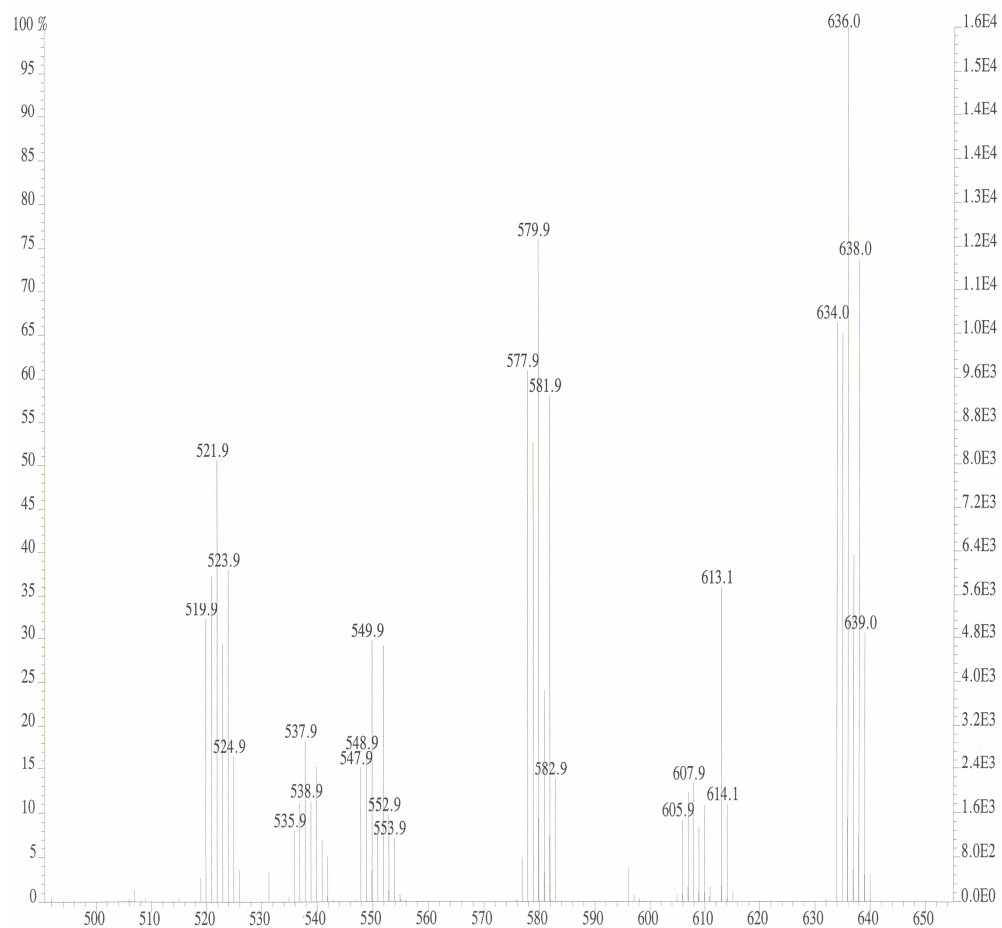


Figure 4.20. Mass spectrum of $W(CO)_4(fcbpy)$.

The UV-VIS spectrum of the complex is displayed in Figure 4.21. There are five absorption bands at 230, 250, 308, 372 and 468 nm. Bands at 230 and 250 nm are assigned to the charge transfer transitions of the ferrocenyl moiety. The band at 308 nm belongs to d-d transition band of 5d electron of $W(0)$. Finally,

there exists the d-d transition of 3d electron of the Fe(II) metal at 372 nm and 468 nm. It is seen that after coordination to a metal, one of the charge transfer bands of the ligand which is at 286 nm shifts to higher energy whereas the d-d transition of Fe(II) metal at 354 shifts to lower energy. The UV-VIS spectra of the free fcbpy molecule and the complex are shown together in Figure 4.22. The molar absorptivities(ϵ) of each absorption band are calculated for the $W(CO)_4(fcbpy)$. According to Beer's law, $A = \epsilon bc$ where b is the cell length in centimeters and c is the concentration of the complex solution in moles per liter. Cell length is taken as 1 cm. Four different concentrations were prepared for the measurements as 1×10^{-5} , 2×10^{-5} , 3×10^{-5} , 5×10^{-5} mol/L. The calculated molar absorptivities are given in Table 4.8.

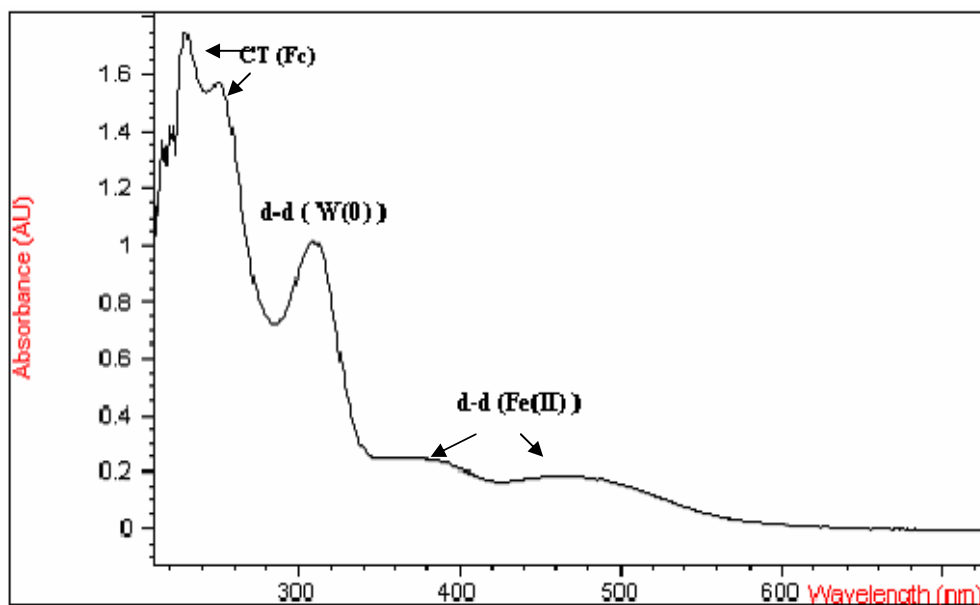


Figure 4.21. The UV-VIS spectrum of $W(CO)_4(fcbpy)$ in CH_2Cl_2 , taken at room temperature.

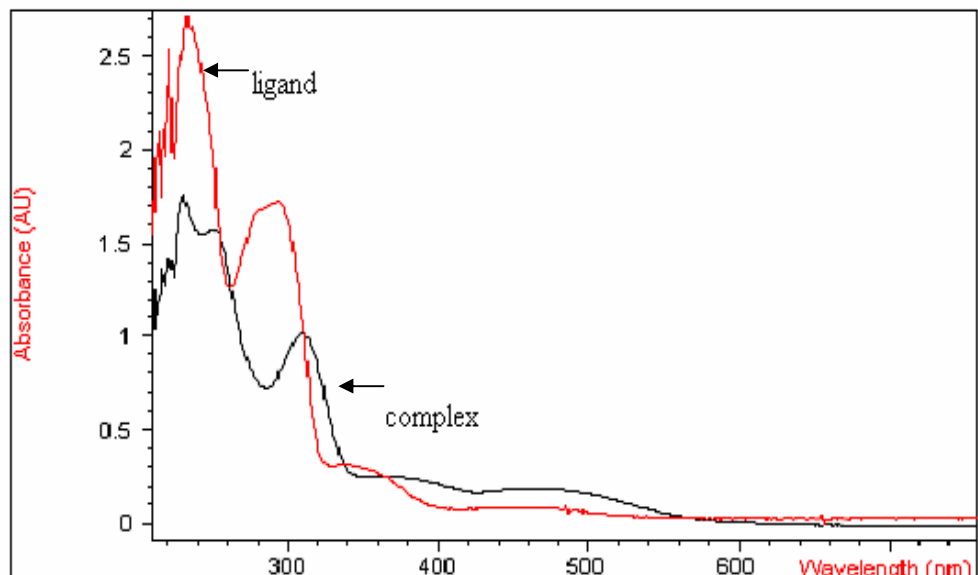


Figure 4.22. The UV-VIS spectra of ligand and complex together in CH_2Cl_2 , taken at room temperature.

Table 4.8. The molar absorptivity values for each absorption band in $\text{W}(\text{CO})_4(\text{fcbpy})$

Absorption Bands (nm)	Molar Absorptivity, ϵ ($\text{Lmol}^{-1}\text{cm}^{-1}$)
230	41700
250	37000
308	24300
372	7500
468	6000

The cyclic voltammogram of $\text{W}(\text{CO})_4(\text{fcbpy})$ given in Figure 4.23 shows a reversible peak readily assigned to the bipyridine moiety: An oxidation at -1.44 V and a reduction at -1.63 V. Then, an irreversible oxidation at 0.519V is

observed which may be assigned to the oxidation of the tungsten metal center from W^0 to W^{1+} . The second oxidation at 0.716V is also irreversible and belongs to tungsten metal center from W^{1+} to W^{3+} . These assignments are based on the comparison with the cyclic voltammogram of a similar complex $W(CO)_4(bpy)$ which has two irreversible oxidations belong to tungsten center at 1.02V and 0.53 V and reversible reduction for bipyridine moiety at -1.58V.⁵⁶ Lastly, the oxidation at 0.871V and reduction at 0.667V are assigned to Fe center from Fe^{+2} to Fe^{+3} based on the comparison to cyclic voltammogram of free fcbpy molecule. The oxidation of ferrocene moiety in $W(CO)_4(fcbpy)$ is observed at more positive potential when compared to free fcbpy molecule. This shift could be attributed to the electron withdrawing property of $W(CO)_4$ moiety which makes the iron center slightly more difficult to oxidize than that of free fcbpy ligand.

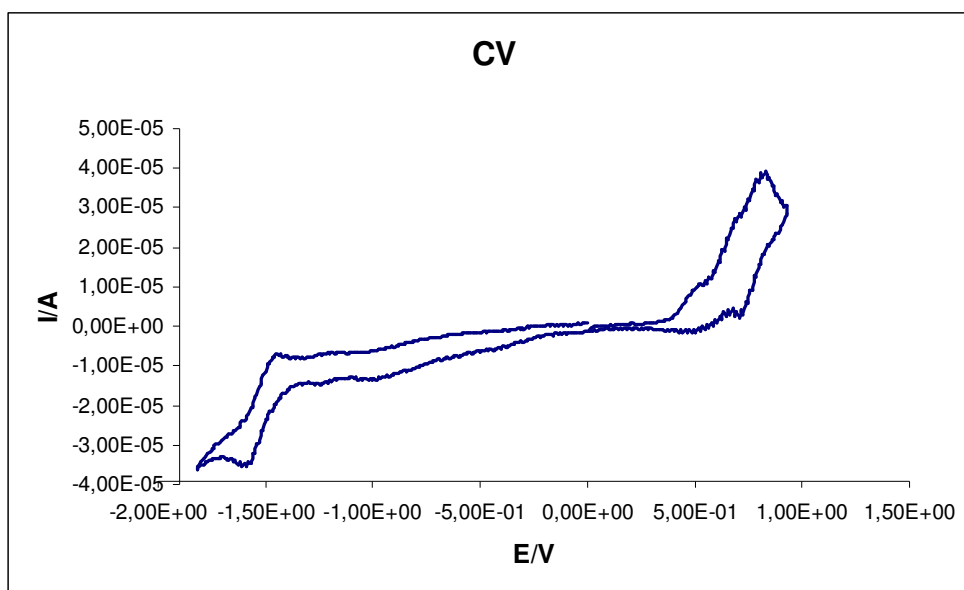


Figure 4.23. Cyclic voltammogram of $W(CO)_4(fcbpy)$ in CH_2Cl_2 at room temperature. Electrolyte; tetrabutylammonium tetrafluoroborate. Reference electrode: SCE

The three oxidations belong to tungsten and Fe centers can be seen more clearly in the expanded cyclic voltammogram given in Figure 4.24.

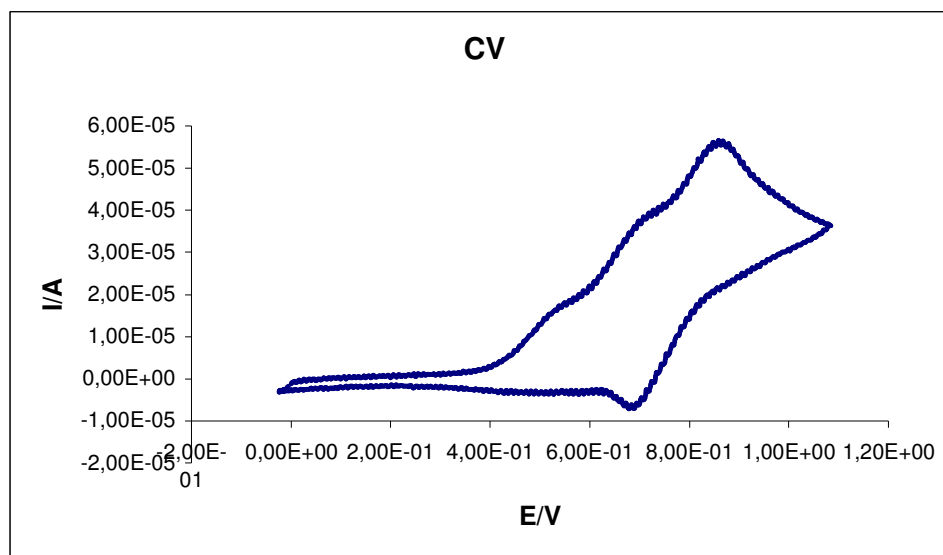


Figure 4.24. Cyclic voltammogram of $W(CO)_4(fcbpy)$ in 1100mV-0mV Electrolyte; tetrabutylammonium tetrafluoroborate. Reference electrode: SCE

The electrochemical oxidation of $W(CO)_4(fcbpy)$ was carried out in CH_2Cl_2 solution and $-21^\circ C$ in order to prevent decomposition of the complex and to minimize the volatilization of the solvent. The spectral changes were recorded in-situ by UV-VIS spectrophotometer. The UV-VIS absorption spectra recorded during electrolysis are shown in Figure 4.25. Although, four electron transfers were expected, the experiment could be carried out until the third electron passage due to the instability of the complex in the solution.

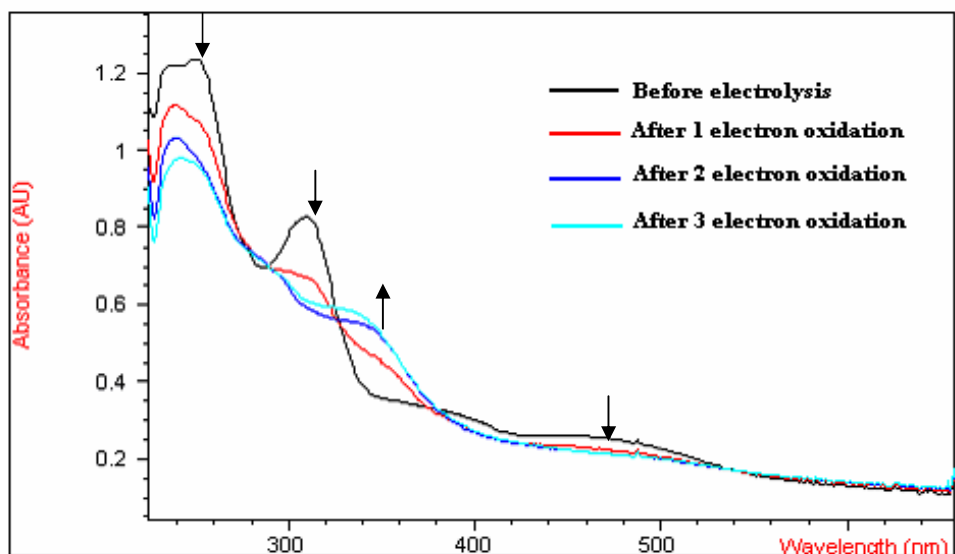


Figure 4.25. The UV-VIS electronic absorption spectra of 1×10^{-4} M $W(CO)_4(fcbpy)$ at -21 °C, recorded during electrolytic oxidation of the complex in CH_2Cl_2 solution containing the electrolyte, 0.1M tetrabutylammonium tetrafluoroborate

In the first electron passage, the absorption bands at 237 nm, 250 nm and 308 nm started to decrease in intensity and a band at 350 nm appeared as shown in Figure 4.26. The observation of isobestic points at 328 nm, 274 nm, 290 nm and 370 nm indicates the straightforward conversion of the complex to the products without any side products. Between the first and second electron transfer the isobestic points get worse except the one at 328 nm. Until second electron passage, all bands continued to decrease in intensity while the intensity of the one at 350 nm increases. At the end of the third electron transfer, the isobestic point could still be observed at 328 nm, however it was not as clear as at the beginning of the experiment.

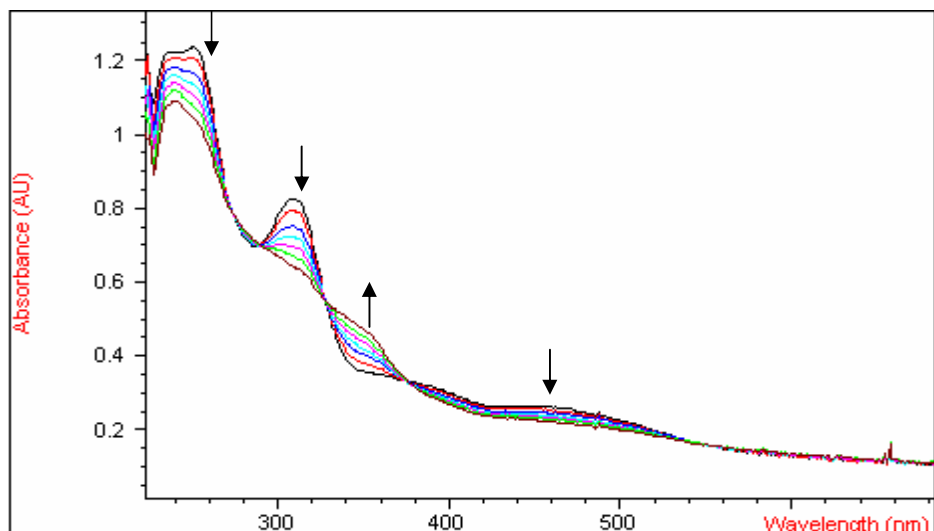


Figure 4.26. The UV-VIS electronic absorption spectra of 1×10^{-4} M $W(CO)_4(fcbpy)$ at -21 °C, recorded after second electron passage of the complex in CH_2Cl_2 solution containing the electrolyte, 0.1 M tetrabutylammonium tetrafluoroborate

4.3. Attempt to synthesize tetracarbonyl(6-ferrocenyl-2,2'-bipyridine) chromium(0)

For the synthesis of $Cr(CO)_4(fcbpy)$, firstly $Cr(CO)_5(THF)$ was prepared by the irradiation of $Cr(CO)_6$ in THF. The course of the reaction was followed by IR spectra taken for every 20 minutes. Since THF is an easily coordinated ligand, so if it is irradiated longer than one hour, the product immediately became $Cr(CO)_4(THF)_2$. So the reaction was stopped after 80% conversion of $Cr(CO)_6$ to $Cr(CO)_5(THF)$. Then, fcbpy ligand was added into the solution in 1/1 molar ratio. The substitution reaction was followed by IR spectra for ten days. After the formation of the desired complex was observed in the spectra, the reaction solution was dried under vacuum. However, the NMR spectra of the complex could not be taken. So, column chromatography was performed in order to get rid off the impurity. Unfortunately, the complex did not go forward through column

although several solvents were applied as eluents. Thus, the solution IR spectrum provides the sole information indicating the formation of $\text{Cr}(\text{CO})_4(\text{fcbpy})$.

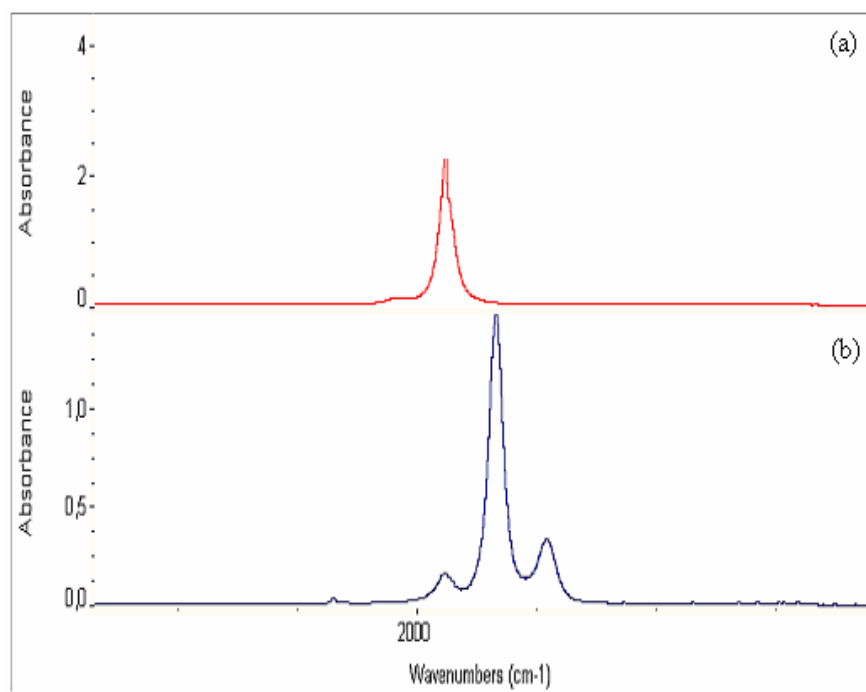
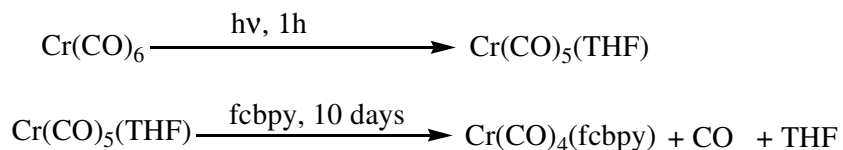


Figure 4.27. The IR spectra taken during irradiation of $\text{Cr}(\text{CO})_6$ in tetrahydrofuran (THF).

- (a) The IR spectrum of $\text{Cr}(\text{CO})_6$.
- (b) The IR spectrum of $\text{Cr}(\text{CO})_5(\text{THF})$

Figure 4.27(a) shows the IR spectrum of $\text{Cr}(\text{CO})_6$ giving an absorption band at 1979 cm^{-1} for CO stretching. Figure 4.27(b) shows the IR spectrum after one hour irradiation indicating the formation of $\text{Cr}(\text{CO})_5(\text{THF})$. The peaks are

2072, 1937 and 1894 cm^{-1} . Figure 4.28 exhibits the course of ligand substitution reaction of $\text{Cr}(\text{CO})_5(\text{THF})$ with fcbpy in THF. The absorption bands at 2072, 1937 and 1894 cm^{-1} of the $\text{Cr}(\text{CO})_5(\text{THF})$ complex are gradually replaced by the new bands at 2006, 1893, 1879 and 1828 cm^{-1} of the $\text{Cr}(\text{CO})_4(\text{fcbpy})$ complex along with the absorption band at 1980 cm^{-1} due to $\text{Cr}(\text{CO})_6$. The absorption bands observed at 2006, 1893, 1879 (as a shoulder) and 1828 cm^{-1} indicate a local C_{2v} symmetry with CO stretching modes of $2A_1 + B_1 + B_2$ for the $\text{Cr}(\text{CO})_4(\text{fcbpy})$ complex. The CO stretching modes and frequencies of both complexes $\text{Cr}(\text{CO})_4(\text{fcbpy})$ and $\text{W}(\text{CO})_4(\text{fcbpy})$ are listed in Table 4.9 for comparison.

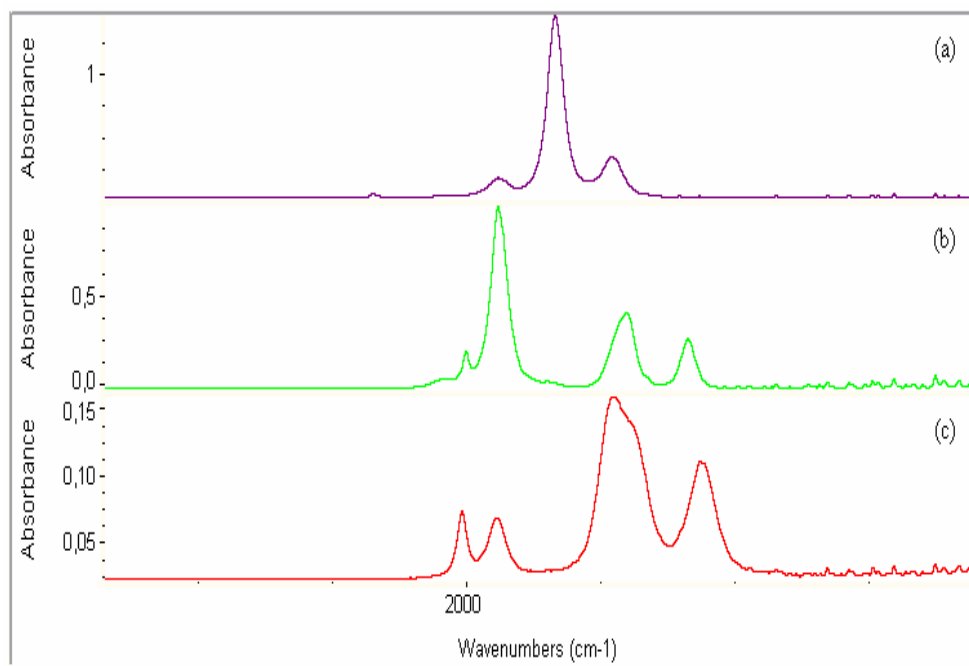


Figure 4.28. The IR spectra taken during substitution reaction of $\text{Cr}(\text{CO})_5(\text{THF})$ with fcbpy.

- (a) The IR spectrum of $\text{Cr}(\text{CO})_5(\text{THF})$ in THF.
- (b) The IR spectrum taken 24h later after starting the substitution reaction in THF.
- (c) The IR spectrum at the end of the substitution reaction in CH_2Cl_2 .

Table 4.9. Vibrational modes and frequencies (cm^{-1}) of $\text{Cr}(\text{CO})_4(\text{fcbpy})$ and $\text{W}(\text{CO})_4(\text{fcbpy})$ in CH_2Cl_2 .

Vibrational Modes	$\text{Cr}(\text{CO})_4(\text{fcbpy})$	$\text{W}(\text{CO})_4(\text{fcbpy})$
A_1^2	2006	2005
B_1	1893	1884
A_1^1	1879	1870
B_2	1828	1823

CHAPTER 5

5. CONCLUSION

The bidentate ligand, 6-ferrocenyl-2,2'-bipyridine (fcbpy) was prepared by the reaction of lithiated ferrocene with bipyridine. Then, it is characterized by ^1H , ^{13}C - NMR, HMQC, and UV-Vis spectroscopies. Furthermore, the electrochemical properties of fcbpy were studied with cyclic voltammetry and controlled potential electrolysis combined with UV-Vis. Cyclic voltammogram exhibits one irreversible reduction belongs due to the bipyridine moiety and a reversible oxidation of ferrocene moiety.

^1H -NMR and ^{13}C - NMR studies enable us to suggest a structure for the fcbpy molecule. The two pyridyl rings are tilted with respect to each other. Thus, the H-3 and H-3' protons are in the deshielding cone of the neighboring aromatic ring.

$\text{W}(\text{CO})_4(\text{fcbpy})$ was synthesized and isolated for the first time from the ligand substitution reaction of $\text{W}(\text{CO})_5(\eta^2\text{-btmse})$ and fcbpy in CH_2Cl_2 . The complex was fully characterized by means of elemental analysis, UV-VIS, IR, ^1H -NMR, ^{13}C -NMR and Mass spectroscopies. The IR spectra of $\text{W}(\text{CO})_4(\text{fcbpy})$ display four absorption bands for CO stretching indicating that the complex has C_{2v} local symmetry for the $\text{W}(\text{CO})_4$ moiety. Thus, the $\text{W}(\text{CO})_4(\text{fcbpy})$ complex has four CO stretching modes of $2\text{A}_1 + \text{B}_1 + \text{B}_2$, all of which are IR active. The local C_{2v} symmetry was also supported by ^1H -NMR and ^{13}C -NMR spectroscopies.

Electrochemical studies of $W(CO)_4(fcbpy)$ started with examining the anodic region. First, the oxidation of tungsten center occurs to W^+ . Next, the tungsten center is oxidized from W^+ to W^{3+} . Thirdly, ferrocene center is oxidized. After that, the reversible reduction of bipyridine moiety was observed in the cathodic region. In other words, four electron passages happen. However, in the electrolysis, only three electron passages could be followed.

When $W(CO)_4(fcbpy)$ complex is compared with $W(CO)_5(2\text{-ferrocenyl pyridine})$ which has already been synthesized,²⁶ it is easily recognized that tetracarbonyl complex is more stable due to the ligand preference. 2,2'-bipyridine, having two nitrogen donor atoms separated by two carbons, forms five-membered rings upon coordination to a transition metal center. π -Electron density is delocalized over the chelate ring via the metal-diimine bonding.

The analogous chromium complex, $Cr(CO)_4(fcbpy)$ was also attempted to be synthesized by the ligand substitution reaction of $Cr(CO)_5(THF)$ and $fcbpy$ in THF. The course of the reaction was followed by taking the IR spectrum. The IR spectrum solution indicates the formation of $Cr(CO)_4(fcbpy)$ complex which exhibits four absorption bands for CO-stretching at frequencies very similar to those of $W(CO)_4(fcbpy)$. However, the chromium complex could not be isolated from the reaction solution due to its instability.

REFERENCES

- ¹ Bochman, M.; Organometallics-1-Complexes with Transition Metal-Carbon σ -bonds; Oxford University Press, Oxford, 1994.
- ² Zeise, W. C.; Pogg. Ann. Phys. Chem., 9,(1827), 632.
- ³ Salzer, A.; Elschenbroich, C.; Organometallics, A Concise Introduction, Second Revised Edition, 1992.
- ⁴ Mond, L.; and Langer, C.; Quinke, F. J.; Chem. Soc., (1890), 749.
- ⁵ Mond, L.; Langer, C.; J. Chem. Soc., (1891), 1090; Berthelot, M.; Acad.C. R.; Sci. Paris, (1891), 1343.
- ⁶ Hein, F.; Chem. Ber., (1919), 52, 195.
- ⁷ Kealy, T. J.; Pauson, P.L.; Nature, (1951), 168, 1039.
- ⁸ Wilkinson, G.; Rosenbulum, M.; Whiting, M. C.; Woodward, R. B.; J. Am. Chem. Soc., (1952), 74, 2125.
- ⁹ Mathey, F.; Sevin A.; Molecular Chemistry of the Transition Elements, 1996.
- ¹⁰ Pruchnik, F. P.; Organometallic Chemistry of the Transition Elements, Plenum Pres, New York, 1990.
- ¹¹ Komiya, S.; Synthesis of Organometallic Compunds, John Wiley & Sons Inc., New York, 1998.
- ¹² Heck, R. F.; Organotransition Metal Chemistry, Academic Press, 1974.
- ¹³ Huheey, J.E.; Keiter, R.L.; Inorganic Chemistry-Principles of Structure and Reactivity, 4th Ed., Harpercollins Colledge Publishers, New York, 1993.
- ¹⁴ Braterman, P. S., Metal Carbonyl Spectra, Academic Press, London,1975.
- ¹⁵ Jones, L. H., In 'Advances in the Chemistry of the Coordination Compounds', (S. Kirschner, Ed.), Macmillan, New York, 1961.

- ¹⁶ Cotton, F. A., 'Modern Coordination Chemistry', (Lewis, J., and Wilkins, R. G., Eds), Interscience, New York, 1960.
- ¹⁷ Crabtree, R.H., The Organometallic Chemistry of the Transition Metals, John Wiley & Sons Inc., New York, 1998.
- ¹⁸ Yaman, Ş. Ö.; Esentürk, E.; Kayran, C.; Önal, A. M.; Z. Naturforsch. 57b, (2002), 92-98.
- ¹⁹ Yaman, G., Thesis Dissertation, METU, Department of Chemistry, 2002.
- ²⁰ Forgues, S. F.; Nicot, B. D.; Journal of Photochemistry and Photobiology A: Chemistry 132 (2000) 137-159
- ²¹ Togni, A.; Hayashi, T.; Ferrocenes: Homogeneous Catalysis, Organic Synthesis, Materials Science, VCH, Weinheim, 1995.
- ²² Whittall, I. R.; McDonagh, A. M.; Humphrey, M. G.; Organometallic complexes in non linear optics I. Second-order non-linearities, Adv. Organomet. Chem., 42, (1998), 291.
- ²³ Astruc, D., Electron Transfer and Chemical Process in Transition-Metal Chemistry, VCH, New York, 1995.
- ²⁴ Rühl, E.; Hitchcock, A. P.; J. Am. Chem. Soc., 111, (1989), 5069.
- ²⁵ Haaland, A.; Acc. Chem. Res., 12, (1979), 415.
- ²⁶ Yaman, G.; Kayran, C.; Özkara S.; Transition Metal Chemistry, 30, (2005), 53.
- ²⁷ Bildstein, B.; Malaun, M.; Kopacka, H.; Wurst, K.; Mitterböck, M.; Ongania K. -H.; Oromolla, G.; Zanello, P.; Organometallics, 18, (1999), 4325.
- ²⁸ Lukasser, J.; Angleitner, H.; Schottenberger, H.; Kopacka, H.; Schweiger, M.; Bildstein, B.; Ongania, K. -H.; Wurst, K.; Organometallics, 14, (1995), 5566. and references therein.
- ²⁹ Bildstein, B.; Schweiger, M.; Kopacka, H.; Ongania, K. -H.; Wurst, K.; Organometallics, 17, (1998), 2414.
- ³⁰ Geiger, W. E., Organometallic Radical Processes. In Journal of Organometallic Chemistry Library; Troglor, W. C.; Ed., Elsevier, Amsterdam, 1990.

- ³¹ Kinnunen, T. J. J.; Haukka, M.; Pesonen, E.; Pakkanen, T. A.; J. Organometallic Chem., 655, (2002), 31.
- ³² Vögtle, F., Supramolecular Chemistry An Introduction, John Wiley&Sons, Chichester, 1991.
- ³³ Butler, I. R., Organometallics, 11, (1992), 74.
- ³⁴ Summers, L. A., Adv. Heterocycl. Chem. 35, (1984), 281.
- ³⁵ Carugo, O.; De Santis, G.; Fabbrizzi, L.; Lichelli, M.; Monichio, A.; Pallavicini, P.; Inorg. Chem., 31, (1992), 765.
- ³⁶ Schlögl, K.; Fried, M.; Monatsh. Chem., 9, (1963), 537.
- ³⁷ Carr, J.D.; Coles, S. J.; Tucker, J. H. R.; Organometallics, (2000), 3312.
- ³⁸ Connely, N.G.; Geiger, W. E; Advances in Organometallic Chemistry, Academic Press, New York, 23, (1984),1.
- ³⁹ Gosser, D. K., Cyclic Voltammetry, VCHVerlagsgesellschaft, New York, 1993.
- ⁴⁰ Shultz, F.A.; Ott, V.R.; Rollison, D.S.; Brovard, D.C.; Mcdonald, J.W. ; Newton, W.E.; Inorg. Chem., 17, (1978),1758.
- ⁴¹ Shriver, D. F.; Atkins, P.W.; Langford, C.H.; Inorganic Chemistry, 2nd Ed., Oxford University Press, New York, 1994.
- ⁴² Solomons, G.; Fryhle, C.; Organic Chemistry, 7th Ed., John Wiley&Sons, Inc., New York, 2000.
- ⁴³ Constable, E., Metals and Ligand Reactivity, VCH Verlagsgesellschaft ,1996.
- ⁴⁴ Dewar, M. J. S.; Bull. Soc. Chim. France , 18, (1951), C71-79.
- ⁴⁵ Chatt, J.; Duncanson, L.A.; J. Chem. Soc., 73, (1953), 2939.
- ⁴⁶ Bayram, E., Master Dissertation, METU, Department of Chemistry, 2004.
- ⁴⁷ Rebiere, F.; Samuel, O.; Kagan, H. B.; Tetrahedon Letters, VOL. 31, No. 22, (1990), 3121.
- ⁴⁸ Butler, I. R.; Roustan, J-L.; Can. J. Chem, Vol. 68, (1990), 2212.
- ⁴⁹ Saldamlı S., Doctoral Dissertation, METU, Department of Chemistry; 2001.
- ⁵⁰ Fish, R. W.; Rosenblum, M.; J. Org. Chem., 30, (1965), 1253.

- ⁵¹ Arnold, R.; Matchett, S. A.; Rosenblum, M.; *Organometallics*, 7, (1988), 2261.
- ⁵² Arnold, R.; Foxman, B. M.; Rosenblum, M.; Euler, W. B.; *Organometallics*, 7, (1988), 1253.
- ⁵³ Schofeld, K., *Hetero-Aromatic Nitrogen Compounds, Pyrroles and Pyridines.*, Butterword and Co., Ltd, London, 1967.
- ⁵⁴ Butler, I. R.; Burke, N.; Hobson, L. J.; Findenegg, H.; *Polyhedron Letters*, No. 19., (1992), 2435.
- ⁵⁵ Marie-Madeleine Rohmer et al.; *Chemical Physics Letters*, 29 (1974), 466.
- ⁵⁶ Crutchley, R. J.; Lever, A. B. P.; *Inorg. Chem.*, 21, (1982), 2276.
- ⁵⁷ Kavaklı C., Thesis Dissertation, METU, Department of Chemisty, 2005.